SEPTEMBER 8-10, 2021
BUDVA, MONTENEGRO

ICONST NST'21

NATURAL SCIENCE

4th INTERNATIONAL CONFERENCE ON NATURAL SCIENCE AND TECHNOLOGY

www.iconst.org

Proceedings & Abstracts Book

ICONST NST 2021

International Conferences on Science and Technology

Natural Science and Technology

September 8-10 in Budva, MONTENEGRO

ABSTRACTS
&
PROCEEDINGS BOOK

ICONST NST 2021

International Conferences on Science and Technology

Natural Science and Technology

September 8-10 in Budva, MONTENEGRO

Editors

Dr. Mustafa Karaboyacı
Dr. Kubilay Taşdelen
Dr. Abdullah Beram
Dr. Hamza Kandemir
Dr. Ergin Kala
MSc. Serkan Özdemir

Technical Editors

MSc. Tunahan Çınar
MSc. Şerafettin Atmaca
MSc. Doğan Akdemir
Ma. Fıratcan Çınar

Cover design & Layout

MSc. Kubilay Yatman

Copyright © 2021

Published by

Association of Kutbilge Academicians, Isparta, Turkey
E-Mail: info@kutbilge.org

Publication Date: 28/09/2021
ISBN: 978-605-70965-0-0

ICONST NST 2021

International Conferences on Science and Technology

Natural Science and Technology

September 8-10 in Budva, MONTENEGRO

Scientific Honorary Committee

Organizing Committee

Technical Committee

ICONST NST 2021

International Conferences on Science and Technology

Natural Science and Technology

September 8-10 in Budva, MONTENEGRO

Scientific Committee

ICONST 2021

International Conferences on Science and Technology

Engineering Science and Technology

Life Science and Technology

Natural Science and Technology

September 8-10, 2021 in Budva, MONTENEGRO

Dear Readers;

The fourth of ICONST organizations was held in Budva/Montenegro between 8-10 September 2021 with the theme of '***science for sustainable technology***' again. In recent years, weather changes due to climate change have reached a perceptible level for everyone and have become a major concern. For this reason, scientific studies that transform technological progress into a sustainable one is seen as the only solution for humanity's salvation. Here we ask ourselves "which branch of science is responsible for sustainability?". Sustainability science is an interdisciplinary field of study that covers all basic sciences with social, economic, ecological dimensions. If we consider technology as the practical application of scientific knowledge, the task of scientists under these conditions is to design products that consume less energy, require less raw materials, and last longer.

ICONST organizations organize congresses on sustainability issues of three main fields of study at the same time in order to present different perspectives to scientists. This year, 157 papers from 28 different countries presented by scientists in **ICONST Organizations**.

85 papers from 17 countries presented in our **International Conference on Engineering Science and Technology** organized under ICONST organizations. Turkey leads the way with 49% of the participants, followed by Kosovo and Moldova with 8.2%, North Macedonia 4.7%, Algeria, Azerbaijan, Hungary, Italy, Montenegro and Poland 3.5%, Croatia, Czech Republic, Kingdom of Saudi Arabia, Japan, Kyrgyzstan, Portugal and Russia with 1.2%.

57 papers from 13 countries presented in our **International Conference on Life Science and Technology** organized under ICONST organizations. Turkey leads the way with 49% of the participants, followed by Poland with 12.7% and Kosovo 11%, United Kingdom 5.4%, Kazakhstan, USA, Tunisia and Croatia 3.6%, Serbia, Israel, Czech Republic and Montenegro with 1.8%.

Finally,15 papers from 8 countries presented in our **International Conference on Natural Science and Technology** organized under ICONST organizations. Turkey leads the way with 47% of the participants, followed by Kosovo with 11% and Serbia, Egypt, Bosnia and Herzegovina, Italy, Poland, North Macedonia and Romania with 6%.

As ICONST organizations, we will continue to organize organizations with the value you deserve in order to exchange ideas against the greatest threat facing humanity, to inspire each other and to contribute to science. See you at future events.

ICONST Organizing Committee

ICONST NST 2021

International Conferences on Science and Technology

Natural Science and Technology

September 8-10 in Budva, MONTENEGRO

Contents

International Conferences on Science and Technology
Natural Sciences and Technology
ICONST NST 2021

Isolation and Characterization of Saponins From Astragalus strictispinis

Rabia Nur Ün[1]*, Tamer Karayıldırım[1], Özgen Alankuş[1]

Abstract: Astragalus L. (Fabaceae) is one of the largest genera of flowering plants with more than 5000 species divided into 269 taxonomic sections. It is represented in the flora of Turkey by 447 species, of which 224 are endemic. Several Astragalus species are used worldwide in traditional medicine as antiperspirants, diuretics, tonics, in the treatment of nephritis, diabetes, leukemia and uterine cancer. Astragalus species are known to be rich in two major classes of biologically active compounds, polysaccharides and saponins. Also the indolizidine alkaloids, the nitro compounds and flavonoids were isolated from the genus.

Astragalus strictispinis (Endemic; Section: Pterophorus) was collected from Burdur, Turkey in 2010. Air-dried and powdered plant material of Astragalus strictispinis was extracted with MeOH. This residue was suspended in H_2O and successively partitioned with n-Hexane, CH_2CI_2 and n-BuOH saturated with H_2O. The n-BuOH phase was chromatographed over column chromatography. The fractions repeatedly subjected to normal phase silica gel CC and reverse phase silica gel column chromatography.

This is the first study that describes the isolation and identification of secondary metabolites from Astragalus strictispinis. In this study, eight cycloartane type glycosides (ASP1-ASP8), 20,25-epoxy-3β-(β-D-xylopyranosyl)oxy-6α-(β-D-glucopyranosyl) oxycycloartane-16β,24α-diol, (ASP 1), 20R,25-epoxy-24S-cycloartane-3β,6α,16β,24-tetraol 3-O-β-D-xylopyranoside-6,24-di-O-β-D-glucopyranoside (ASP 2), 3-O-β-D-xylopyranosyl-6-O-β-D-glucopyranosyl-(20R,24S)-epoxy-3β,6α,16β,25-tetrahydroxy cycloartane (ASP 3), 3β,6α,16β,25-tetrahydroxy-20(R),24(S)-epoxycycloartane (ASP 4), 3,6-di-O-β-D-xylopyranosyl-3β,6α,16β,24(S),25-pentahydroxycycloartane (ASP 5), 6-O-β-D-glucopyranosyl-3β,6α,16β,25-tetrahydroxy-20(R),24(S)-epoxycycloartane (ASP 6), 3-O-β-D-xylopyranosyl-3β,6α,16β,24α-tetrahydroxy-20(R),25-epoxycycloartane (ASP 7), 3β,6α,16β,24α-tetrahydroxy-20(R),25-epoxycycloartane (ASP 8) were isolated from the methanolic extract. Their structures were elucidated by extensive spectroscopic methods including 1D- and 2D-NMR techniques.

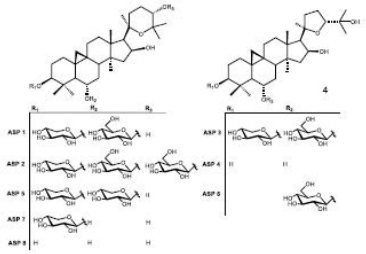

Keywords: Fabaceae, Astragalus, Secondary metabolities, Saponins.

Acknowledgements: The authors are greatful to TUBITAK (117Z572), for the financial support.

· Ege University, Faculty of Science, Department of Chemistry, Izmir, Turkey.
* Corresponding author: rabia.nur.un@ege.edu.tr

International Conferences on Science and Technology
Natural Sciences and Technology
ICONST NST 2021

Evaluation of Physicochemical Properties of Swimming Pool Waters in Prizren Province, Republic of Kosovo

Cengiz Cesko[1]*, Dijar Latifi[2], Erva Halce[3]

Abstract: Swimming is a popular recreational physical activity today. In this respect, it is necessary that the physico-chemical data of swimming pools comply with international standards in terms of human health. The construction of many swimming pools in Kosovo in recent years has caused the public to attach great importance to swimming. However, having hygienically clean and safe areas is important for public health. Ensuring the quality of the water, which is exposed during swimming, in accordance with the standards in terms of physical, chemical and biological standards, is the most decisive factor in making hygiene sustainable.

In this study, pH, TDS, turbidity, temperature, odor and water hardness analyzes were made from pool water samples collected from various parts of Kosovo. After the pool water analysis was done, it was compared with the tap water analysis. As a result of the study, it was seen that the pool waters had a pH value of approximately 8 with tap water. The hardness level of the tap water is 8 and although it is of medium hardness, the hardness level of the pool water is approximately 30 due to the chemicals it normally contains. The TDS value of the tap water is 90 ppm, and the TDS values of the pool waters are between 280 ppm and 320 ppm. It has been determined as a result of experimental data that increasing the pH value decreases the active chlorine ratio.

Keywords: Swimingpool, physico-chemical analys, water.

[1]University of Bussines and Technology, Departament of Food Science and Biotechnology – Prisitina – Kosovo
[2]Ankara University, Department of Fisheries, Ankara, Turkey
[3]Uludag University, Department of Chemistry, Bursa, Turkey
* Corresponding author: cengizchesko@hotmail.com

International Conferences on Science and Technology
Natural Sciences and Technology
ICONST NST 2021

Assessment of the Impact of Industrial Wastewater Pollution on The Receiving Water Quality

Joanna Boguniewicz-Zabłocka[1]*, Iwona Kłosok-Bazan[1], Mustafa Karaboyacı[2]

Abstract: Water is the basis of life on earth, which is why it's protection is so important. Man through his activity poses a threat to both its resources and quality. The pressures exerted on the waters are primarily related to the emission of municipal and industrial wastewater from sewage treatment plants, as well as entering the waters as surface runoff - diffuse pollution. Point and non-point sources pollution of surface waters can have a significant impact on the physicochemical state of the receiver.

This article presents an assessment of the impact of industrial wastewater pollution outflow into the river. The impact of wastewater treatment processes used in the industry was taken into account. The main causes of river pollution have been identified. In the analysis, particular attention was paid to pollution expressed by indicators: BOD, COD and suspended solids.

Keywords: industrial wastewater, environmental pollution, BOD, COD, suspended solids.

[1] Opole University of Technology, Faculty of Mechanical Engineering, Department of Thermal Engineering and Industrial Facilities, Opole, Poland
[2] Süleyman Demirel University, Engineering Faculty, Chemical Eng. Department, Isparta, Turkey
* Corresponding author: j.boguniewicz@po.opole.pl

International Conferences on Science and Technology
Natural Sciences and Technology
ICONST NST 2021

Qualitative Composition of Macrozobenthos from Lisolaj, Mavrovo, Nikiforovo and Leunovo River

Radmila Ilieska[1*] ,Stoe Smiljkov, Mila Mandikj

Abstract: From the research of the macrozoobenthos from the rivers that flow into Mavrovo Lake conducted in the examined period 2016 - 2018, after the qualitative analysis of the samples collected from four different localities: Mavrovo River, Nikiforovo River, River Lisolaj and Leunovo River, we determined the presence of 12 different groups: Turbellaria (flatworms), Gastropoda (snails), Hirudinea (leeches), Crustacea (crabs), Ephemeroptera (mayflies), Plecoptera (stoneflies), Hemiptera (true bugs), Trichoptera (caddisflies), family Chironomidae (non-biting midges), family Simulidae (black flies), family Dixidae (meniscus midges) and family Elmidae (riffle beetles). The most common group in the entire examined period was the order Ephemeroptera from the class Insecta (insects). Mavrovo River is characterized by the greatest diversity and 10 groups were identified at this location. The summer season was characterized by the greatest diversity and 11 groups of macroinvertebrates were recorded. The orders Ephemeroptera (90%) and Plecoptera (80%) and the class Hirudinea (80%) stand out as euconstant groups. Mavrovo River and Nikiforovo River are characterized by the highest faunal similarity (84,62%), while Mavrovo River and River Lisolaj (40%) are characterized with lowest Sørensen Coefficient.

Keywords: macrozoobenthos, rivers, qualitative composition

[1] Institute of Biology, Faculty of Natural Science and Mathemathics, 1000 Skopje, R. Macedonia
* Corresponding author: ilieskar@yahoo.com

International Conferences on Science and Technology
Natural Sciences and Technology
ICONST NST 2021

New Functional ZnO Nanoparticle –Based Coatings with Antibacterial Properties Synthesizes By A Facile Microwave Approach

Maria Antonia Tănase[1], Adina Răducan[1], Petruţa Oancea[1], Cristina Lavinia Nistor[2], Elvira Alexandrescu[2], Cristina Scomoroscenco[2], Cristian Petcu[2], Maria Marinescu[3], Lia Mara Diţu[4] , Ludmila Otilia Cinteză[1*]

Abstract: As the use and availability of superhydrophobic materials has increased, so has the demand of more simple, low cost and environmental friendly alternatives to produce them. Nanostructured materials that are simultaneously superhydrophobic and poses self-cleaning, antibacterial and anti-corrosion proprieties, are required to obtain multifunctional textiles.In this work a facile fabrication of superhydrophobic textiles based on a microwave synthesis of ZnO nanoparticles and further modification with non-fluorinated silane coatings (alkyl trimethylsiloxane or polysiloxanes). $Zn(NO_3)_2$ and NaOH precursors were used in order to obtain the ZnO nanoparticles needed. By fine tuning the parameters of the hydrothermal reaction (time, temperature, and compound ratios) multiple variants were obtained for the ZnO nanoparticles, which were then analyzed using DLS, XRD and SEM. This allowed us to characterize said nanoparticles by size, size distribution, crystalinity and morphology.Hybrid films were deposited on cotton as textile model surfaces. The cellulosic materials previously modified with Chitosan provide a stable base on which the ZnO nanoparticles and organomodified silane derivative can be applied. Water contact angles were measured in order to evaluate the wettability of the ZnO nanoparticle-based coating. The contact angles ranged from 147 to 153^0, which support the highly hydrophobic and superhydrophobic properties of the tested coatings.The bacteriostatic activity of the ZnO nanoparticles was proven to be highly efficient on treated textile substrates, even la very low concentrations.In conclusion, owning to the hydrophobic, bacteriostatic and non-toxic proprieties of the suggested microwave synthesized material, this could serve as a viable multifunctional coating with multiple applications, for example protecting modern textile and historical artifacts from weathering damage and biofilm formation or improving the antiseptic qualities of bio-medical devices.

Keywords: This work was supported by grants of the Romanian Ministery of Research and Innovation, CCCDI - UEFISCDI, project number PN-III-P1-1.2-PCCDI-2017-0743/P5, within PNCDI III, contract 44PCCDI/2018, within PNCDI III.

[1]University of Bucharest, Physical Chemistry Department, 4-12 Elisabeta Blvd, Bucharest, Romania;
[2]INCDCP-ICECHIM, Polymer Department, 202 Splaiul Independentei, Bucharest, Romania
[3]University of Bucharest, Organic Chemistry, Catalysis and Biochemistry Department, 92 Panduri Blvd, Bucharest, Romania
[4]University of Bucharest, Department of Microbiology and Immunology, 1-3 Aleea Portocalelor, 060101, Bucharest, Romania
* Corresponding author: ocinteza@yahoo.com

International Conferences on Science and Technology
Natural Sciences and Technology
ICONST NST 2021

The Effect Of Climate Change On The Distribution Of Some Bird Species

Yasemin Öztürk[1*]

Abstract: Birds choose their nesting sites based on many criteria. These criteria are an abundance of food, safe place to lay eggs. The ecological conditions required during the breeding season are species-specific and complex. In recent years, changes have occurred in the breeding areas of birds with the effect of global warming. This study was carried out in the province of Burdur, where this change was experienced, in 2019 and 2021. Within the scope of the study, 4 species in Burdur were investigated; Spilopelia senegalensis, Phoenicopterus roseus, Recurvirostra avosetta, Vanellus spinosus. The first breeding record of the Laughing Dove, which is an invasive species, in Burdur was determined by us in March 2019 in Gölhisar. Large numbers of Greater Flamingo and Pied Avocet flocks were identified during fieldworks in July 2021. Both species had juvenile. In Burdur and Karataş lakes, in July 2021, 98 individuals of Vanellus spinosus species were counted and it was determined that some individuals were incubating and having juvenile. Recurvirostra avosetta and Phoenicopterus roseus counted 333 and 4321 individuals, respectively. The breeding areas of these three species living in marsh, brackish or salt waters have expanded. Especially with the withdrawal of lake waters as a result of the increase in temperature, the marsh area increased and attracted the species that prefer these areas. In addition, the Laughing Dove, which provides a suitable living environment with an increase in temperature, increases its spread by invading new areas like Burdur.

Keywords: Burdur Lake, Climate change, *Spilopelia senegalensis*, *Vanellus spinosus*, *Phoenicopterus roseus*, Karataş lake

[1] Burdur Mehmet Akif Ersoy University, Golhisar Vocational School, Department of Forestry, Burdur, Türkiye
* Corresponding author: yyaseminozturk@gmail.com

International Conferences on Science and Technology
Natural Sciences and Technology
ICONST NST 2021

The Impact of Composition of The Members of The Board of Directors on The Fınancıal Performance if Limited Liability Companies in Kosovo

Dafina Abdullahu[1*]

Abstract: Corporate governance is being studied from different perspectives because of the importance to achieve better performance of enterprises. The global financial crisis, corporate scandals and public concern about how companies are run have contributed to increased interest of decision makers. This research aims to explain its influence corporate governance in the financial performance of LLC (**Limited Liability Company)** in Kosovo. The research involved 80 selected LLC's selected from the Tax Administration of Kosovo as a large taxpayers. From the data analysis it appears that the composition of the members of the Board of Directors is a factor that affects the financial performance of enterprises.

Keywords: Corporate governance, financial performance, Board of Directors.

[1] University of Prizren" Ukshin Hoti", Prizren, Kosovo
* Corresponding author: dafina.abdullahu@uni-prizren.com

International Conferences on Science and Technology
Natural Sciences and Technology
ICONST NST 2021

Use of Specialized CAPE-loaded Extracellular Vesicles as a Targeted Approach in Treatment of Neuroblastoma

Ezgi Avşar Abdik[1]*, Hüseyin Abdik[2], P. Neslihan Taşlı[1], Oğuz Kaan Kırbaş[1], Batuhan Turhan Bozkurt[1], Fikrettin Şahin[1]

Abstract: Neuroblastoma is a solid type of tumor originating from primordial neural crest cells that are located in adrenal medulla and sympathic ganglions. Neuroblastoma tumors are frequently encountered in children and they are highly heterogeneous in nature. Emerging studies have demonstrated that microvesicles that are found in the tumor microenvironment as secretory outputs from various types of resident cells play a promoting role in the progression and growth of these types of tumors. Exosomes are known as the smallest member of the superfamily of extracellular vesicles found in the tumor microenvironment. They -typically- consist of proteins that can be derived from the plasma membrane, tetraspanins, and receptors of the cells from which they originate. Display of these proteins on the exosomal periphery facilitates their recognition and subsequent uptake by the recipient cells of the organisms. This property of exosomes has promoted their reputation as efficient messengers of physiological inter-cellular communication web and, hence, enticed a strong interest in investigating the possibility of using them as tools of drug delivery in treatment of human cancer. Numerous naturally existing compounds or their synthetic derivatives are shown to have anti-tumorigenic activities in countless studies over the years. Propolis is one such source for over 300 different types of compounds, one of which is caffeic acid phenethyl ester (CAPE) that has anti-oxidant, anti-neoplastic, anti-inflammatory, anti-tumoral, neuro-protective, and immunomodulatory properties. Moreover, this compound is known to exert anti-angiogenic, anti-metastatic, anti-proliferative effects, while promoting apoptosis in tumor cells. The aim of this study was to investigate the potential tumor-suppressive effects of extracellular vesicles (EVs) -loaded with CAPE in the in-vitro model of neuroblastoma cell line, SH-SY5Y, with a focus on the CAPE-induced changes in apoptotic signaling.

EVs derived from the human dermal neonatal fibroblasts that are induced for neurogenic differentiation and can mimic neuroblastoma cells were loaded with CAPE. Characterization of EVs with nanoparticle tracking system, electron microscopy and flow cytometry analysis were performed with according to MISEV criteria. Cytotoxicity was determined in neuroblastoma cell line SH-SY5Y and healthy cell line HaCaT by MTT assay following 24, 48 and 72 hours. According to the findings a dramatic decrease in tumor cell viability (~20%) was observed when CAPE was delivered as a cargo of EVs compared to conditions of its direct administration as a single agent (~80%) or unloaded EVs in SH-SY5Y cells. Apoptosis rates were determined by Annexin V analysis and Hoechst staining. CAPE-loaded EVs markedly increased apoptotic cell ratio compared to CAPE and unloaded EVs alone in neuroblastoma cell line. Besides, it was observed that RT-PCR results regarding apoptotic signaling genes induced with CAPE treatment support the findings of Annexin V analysis.

[1]Yeditepe University, Faculty of Engineering and Architecture, Department of Genetics and Bioengineering, Istanbul, Turkey
[2]Istanbul Sabahattin Zaim University, Faculty of Engineering and Natural Sciences, Department of Molecular Biology and Genetics, Istanbul, Turkey
*Corresponding author: Ezgi Avşar Abdik; ezgi.avsar@yeditepe.edu.tr

These findings are encouraging to undertake further studies to assess the potential use of CAPE-loaded EVs in treatment of neuroblastoma.

Keywords: Neuroblastoma, Extracellular vesicles, CAPE, CAPE-loaded EVs, Apoptosis**.**

This study is part of Project 119S735, funded by Scientific and Technological Research Council of Turkey (TUBITAK).

International Conferences on Science and Technology
Natural Sciences and Technology
ICONST NST 2021

Investigation of Isophthalic Acid Degradation by *C. testosteroni* Strains

Caner Vural[1*]

Abstract: Phthalates, known as phthalic acid esters, are used as raw materials in the plastics industry. Their accumulation in the environment causes many environmental and health problems. Therefore, rapid and effective removal of these compounds is essential for a sustainable environment and health. Phthalic acid and its isomers are monomers of phthalates. In this study, *Comamonas testosteroni* strains were investigated for their potential catabolic abilities on Isophthalic Acid (IPA). HPLC analyses indicated that *C. testosteroni* strain H1 and *C. testosteroni* strain H2 have the successful degradation ability on IPA. The isolates were completely degraded 101.56 mg/L and 101.58 mg/L of IPA within 8 and 9 hours.

Keywords: *Comamonas testosteroni*, Isophthalic acid, Biodegradation, HPLC

1. Introduction

Plastic-based industrial products are one of the leading products for consumption. The low cost of production and the functionality of the products can be remarked as the main reasons for overproduction. PA isomers and PA esters are widely used in the plastics industry (Vamsee-Krishna and Phale, 2008; Tang et al. 2020). Therefore, PA esters have become one of the most used organic compounds worldwide. For example, it has been reported that 1 million tons or more of PA esters are used annually in Europe and China alone (Tang et al. 2020).

Phthalates are esters of 1,2-benzene dicarboxylic acid (PA). Structurally, it varies according to the number of side chains such as dialkyl, alkyl or aryl groups attached to the basic phenyl moiety (Latini 2005; Liang et al. 2008; Benjamin et al. 2015). 1,2-benzene dicarboxylic acid has three isomeric forms as ortho-isomer (phthalic acid), para-isomer (terephthalic acid) and meta-isomer (isophthalic acid). These forms are used as the main raw material of various products in the plastic industry. Phthalates have been used in various industries since the 1930s (Latin 2005). For example, PA esters are commonly used in the polyvinyl chloride (PVC) industry, while TA esters are used in the production of polyester fibres and polyethene terephthalate (PET). As relatively less used compounds, IPA esters are used to produce dope, resin, etc. (Liang et al. 2008; Benjamin et al. 2015).

Phthalates used in plastic production are not always covalently bonded to polymers, so phthalates can be separated from the polymer structure over time. Therefore, they can be released into the environment in various ways (Liang et al. 2008; Vamsee-Krishna and Phale, 2008; Sawers 2018; Tang et al. 2020). Structural separation can be accelerated by physicochemical factors such as temperature, pressure, pH, presence of solvents, organic compounds, and radiations (Benjamin et al. 2015). By migrating to various environments, these chemical compounds cause many health problems and It is necessary to remove them

[1] Pamukkale University, Faculty of Science & Arts, Department of Biology, Denizli, Turkey
* Corresponding author: canerv@pau.edu.tr

from environmental systems (Latini 2005; Benjamin et al. 2015; Sawers 2018; Wang et al. 2019).

There are several ways to remove phthalates from environmental systems, such as photochemical degradation, hydrolysis, and biodegradation. (Staples et al. 1997; Benjamin et al. 2015). Photochemical degradation and hydrolysis generally occur at slow rates and take a long time. It is also known that acids, bases, metal ions, anions or organic substances mediate these processes (Benjamin et al. 2015). Apart from this, much more energy, extra land and more time may be needed to provide physicochemical degradation processes. On the other hand, biodegradation which is the process done by microorganisms becomes a good option for the removal of such harmful compounds from contaminated sites. It has been reported that the microorganisms play a leading role in the biodegradation of phthalates (Liang et al. 2008; Sawers 2018), and many bacterial strains, some fungi, yeasts and algae may be responsible for the degradation of phthalates under aerobic or anaerobic conditions (Benjamin et al. 2015).

In this study, the degradation of IPA, which is one of the phthalate precursors, was investigated under aerobic conditions with *C. testosteroni* isolates previously isolated from a petrochemical industry wastewater treatment plant.

2. Material and Method

2.1. Microbiological parameters

Firstly, *C. testosteroni* isolates were inoculated into sterile LB medium and incubated on a rotary shaker at 200 rpm, 30°C for 24-48 hours. Then, the isolates were centrifuged at 5000 rpm for 5 minutes, and supernatants were discarded. Subsequently, the isolates were transferred to sterile tubes containing phosphate buffered water (PBS) and homogenated by gently vortexing. Cell densities were adjusted to 0.5 McFarland (MF) units (approximately 1.5 x 108 cells/ml) at a wavelength of 565 ± 15 nm with a densitometer (Den-1B, Grant Instruments, UK). Following, IPA was transferred from the stock solution (2000 mg IPA/1000 ml DMSO) to sterile flasks containing 50 ml of Bushnell Haas liquid medium (supplemented with 0.05% yeast extract) as to be a 100 mg/L in a final concentration. After a short shaking, density adjusted cells were individually inoculated into flasks as to be 5% in a final concentration. The flasks were then started to the incubation for the degradation on a rotary shaker at 200 rpm at 30°C. Samples were taken into 1.5 ml microcentrifuge tubes hourly for analytical measurements by HPLC.

2.2. Analytical measurements

High-Pressure Liquid Chromatography (HPLC) equipped with a vacuum degasser, a quaternary pump, an autosampler, and a diode array detector system (Agilent 1100 series HPLC system, USA) was used to determine the biodegradation activities of the isolates on IPA. Data collection was performed using Chem-Station software (Agilent 1100 series HPLC system, USA) and ZORBAX Eclipse PAH column (4.6×150 mm, 3.5 µm) (Agilent, USA) set at 25°C for analysis was used. The mobile phase was adjusted to acetonitrile + 0.1% Formic acid (A) and water (B). The flow condition was 70:30% of A: B (mobile phase) at a flow rate of 1.0 mL/min. The detection wavelength and retention time were determined at 220 nm, 1.69 minutes, respectively. First, a standard curve plot was created by determining the areas for a series of concentrations. This plot was used to calculate the IPA concentration in the unknown sample. 1 ml of sample was taken from each bottle and centrifuged at 10000 rpm for 5 minutes. Afterwards, the supernatants were taken into HPLC vials and HPLC analyzes were performed.

3. Results

Degradation studies showed that two *C. testosteroni* isolates have actively degraded IPA. It was measured that the *C. testosteroni* isolate H1 has degraded IPA with an initial concentration of 101.58 mg/L to 28.52 mg/L at the 7th hour, while it was observed that IPA was completely depleted in the fermentation liquid at the 8th hour (Figure 1). The degradation efficiencies of the isolate H1 were calculated 71.92% at the 7th hour, and 100% at the 8th hour, respectively (Figure 2). Similarly, *C. testosteroni* isolate H2 has degraded 101.56 mg/L of IPA to 36.85 mg/L in 7 hours, reduced it to 1.88 mg/L at the 8th hour, and completely consumed at the 9th hour (Figure 1). The degradation efficiency of the isolate H2 was calculated as 63.72% at the 7th hour, 98.15% at the 8th hour, and 100% at the 9th hour, respectively (Figure 2).

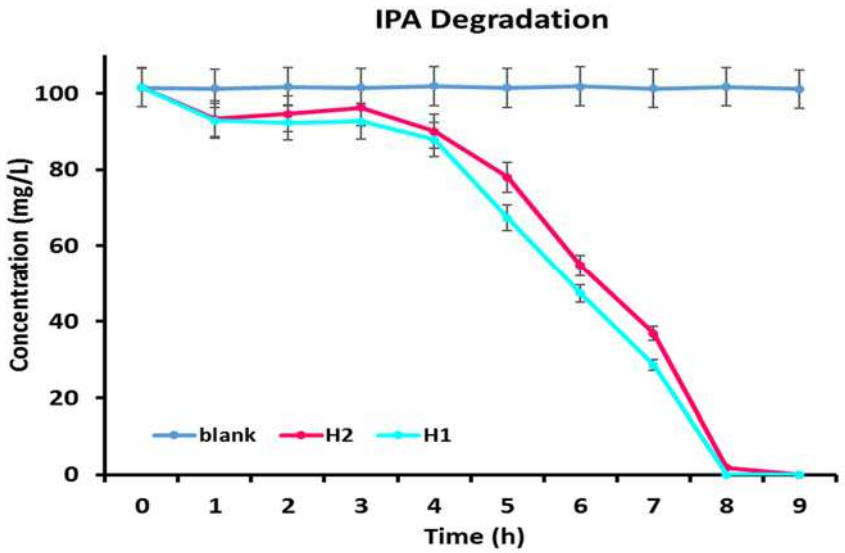

Figure 1. IPA degradation by isolate H1 and H2.

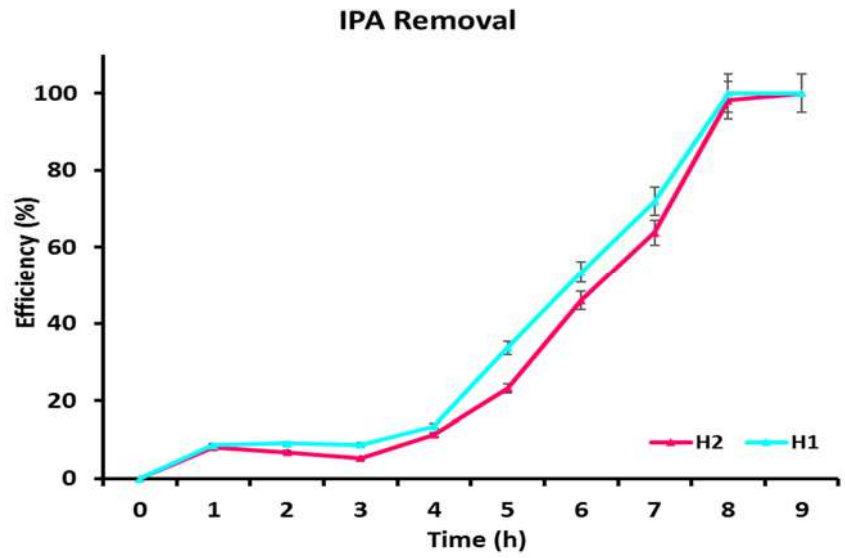

Figure 2. Degradation efficiencies of *C. testosteroni* isolate H1 and H2 on IPA.

4. Discussion and Conclusions

Gram-positive and Gram-negative bacteria have different metabolic pathways to break down phthalates under aerobic and anaerobic conditions. Aerobic phthalate degrading bacteria are generally known as members of *Burkholderia*, *Delftia*, *Sphingomonas*, *Comamonas*, *Pseudomonas*, *Arthrobacter*, *Terrabacter*, *Mycobacterium* and *Rhodococcus* genera (Liang et al. 2008). It has been stated that degradation in aerobic conditions is much faster than in anaerobic conditions (Benjamin et al. 2015). Within these mentioned genera, the members of the *Comamonas* genus have so far received great attention to cope with challenging environmental conditions. Particularly, their ability to degrade complex organic pollutants and their resistance to heavy metals are the biggest factors in attracting attention. They could be good candidates for bioremediation because of their successful adaptation to various environments (Li et al. 2017).
To date, biodegradation of terephthalate and isophthalate in diverse bacteria has been reported. *C. testosteroni* YZW-D metabolizes terephthalate and isophthalate through metabolic pathways in which the tph and iph catabolic genes are involved, respectively. These catabolic genes, which are responsible for cleavage of terephthalate and isophthalate, also have been characterized in *Comamonas sp*. strain E6. In these catabolic pathways, terephthalate and isophthalate are converted to protocatechuate, and protocatechuate is further degraded via 4,5-cleavage (Kasai et al. 2019). In conclusion, within the frame of this study, it could be said that *C. testosteroni* isolate H1 and H2 may be the successful candidates to achieve cleaning the environmental pollution contaminated with IPA.

Acknowledgements

This study was supported as a research project (Project No: 16-Fen-023) by Ege University Scientific Research Projects Coordination Unit. Also, I would like to thank Tayyibe Alpay Uyaniker and Hursel Cay for the supplying of *C. testosteroni* strains from previous studies.

References

Vamsee-Krishna, C., Phale, P.S., (2008). Bacterial degradation of phthalate isomers and their esters. Indian J Microbiol,48, 19–34.

Tang, J., Rong, X., Jin, D., Gu, C., Chen, A., Luo, S., (2020). Biodegradation of phthalate esters in four agricultural soils: Main influencing factors and mechanisms. Int Biodeterior Biodegrad, 147, 104867. doi.org/10.1016/j.ibiod.2019.104867

Latini, G., (2005) Monitoring phthalate exposure in humans. Clin Chim Acta, 361, 20–29.

Liang, D.W., Zhang, T., Fang, H.H.P., He, J., (2008). Phthalates biodegradation in the environment. Appl Microbiol Biotechnol, 80, 183–198.

Benjamin, S., Pradeep, S., Sarath, M., Kumar, S., (2015). A monograph on the remediation of hazardous phthalates. J Hazard Mater, 298, 58–72.

Sawers, R.G., (2018). o-Phthalate derived from plastics' plasticizers and a bacterium's solution to its anaerobic degradation. Mol Microbiol, 108, 595–600.

Wang, Y., Zhu, H., Kannan, K., (2019). A review of biomonitoring of phthalate exposures. Toxics, 7, 1–29.
Staples, A.C., Peterson, D.R., Parkerton, T.F., Adams, W.J., (1997). The environmental fate of phthalate esters: A literature review. Chemosphere, 35(4), 667-749.

Li, J., Luo, F., Chu, D., Xuan, H., Dai, X., (2017). Complete degradation of dimethyl phthalate by a Comamonas testosterone strain. J Basic Microbiol, 57, 941–949.

Kasai, D., Iwasaki, T., Nagai, K., Araki, N., Nishi, T., Fukuda, M., (2019). 2,3-Dihydroxybenzoate meta-Cleavage Pathway is Involved in o-Phthalate Utilization in Pseudomonas sp. strain PTH10. Sci Rep, 9, 1–11.

International Conferences on Science and Technology
Natural Sciences and Technology
ICONST NST 2021

Influences of Hot Plasmas on the Reactor Walls, a BCA Work

Yakup Hundur[1*], Merve İlay Çelikkaya[2]

Abstract: Tungsten is the wall material for the fusion reactor ITER in France. Hydrogen is the major fuel for the fusion reaction due to its abundance on Earth. Collisions of deuterium with the walls result sputtering, reflection, transmission, and structure manipulations on the target. In this study, we introduce the interactions between the Tungsten layer bombarded with Deuterium atoms at energy values 700 eV and 800 eV with varying angles by employing the binary collision approximation (BCA) model. The collisions between the Tungsten target and Deuterium atoms are simulated separately for different angles from 0 ˚ to 89 ˚. The number and the average energies of backscattered and excavated atoms are investigated to enhance the tungsten wall constructions.

Keywords: Fusion plasmas, plasma-wall interaction, Sputtering, BCA model.

1. Introduction

The first experimental fusion reactor ITER and the following pre-commercial DEMO reactors are promising alternatives for energy needs in the future (Lasa, et al., 2014, (Chatzis & Barbarino, 2021). The hydrogen isotopes Deuterium (D) and Tritium (T) is the main fuel of the thermonuclear fusion reactor due to relatively low-temperature levels to reach fusion conditions. Plasma fuel in tokamak reactors is confined and controlled by a strong magnetic field in a toroidal chamber. The uncontrolled neutral particles of the plasma continuously bombard the walls of the reactor (Polvi, et al., 2016). Plasma-facing components (PFCs) are exposed to tremendous temperature, particle flux, and irradiation levels. Significant part of escaping particles of plasma is interacting with the divertor at the bottom of the reactor. (B.D. Wirth, 2011)

Tungsten is chosen as the main material for the reactor due to its low tritium retention and high melting point (Marian, et al., 2017). Degradation due to plasma-surface interactions is an obstacle to commercial use of the tokamak system. Simulating the interactions takes an important role before sophisticated constructions.

Interaction between the plasma and the reactor surface causes sputtering of the wall material, tritium retention, and blistering. Change in the plasma composition due to the sputtered atoms and fuel retention reduces the plasma temperature and hinders the reaction to proceed (Nordlund, et al., 2014). Effects of the incoming projectile on sputtering are studied in both experimental and various computational methods (Taniguchi, et al., 2003, Marian, et al., 2017, (Hundur & Karateke, 2019)).

[1] İstanbul Technical University, Faculty of Science and Letters, Physics Engineering, İstanbul, Türkiye
[2] İstanbul Technical University, Graduate School, Energy Science and Technology, İstanbul, Türkiye
* Corresponding author: hundur@itu.edu.com

In this study, a ready program SRIM which based on binary collision approximation for simulating the colliding particles is used. Excavated Tungsten atoms and backscattered Deuterium ions are presented in terms of incidence and average energies. Ion penetration in the tungsten layer is also investigated.

2. Method

H projectile with mass 2.014 amu on tungsten (W) target is given as input parameters for SRIM. The target layer depth is determined as 1000 Å in order to inhibit the transmission of projectiles through the surface to the bottom. Incident energy of deuterium (D) atoms are chosen as 700 eV and 800 eV. Projectiles are sent to the surface with varying angles between 0˚ to 89 ˚. To get an accurate result, projectiles are iterated million times for two energy levels.

The number and the average energy of the excavated W atoms and the number of backscattered deuterium atoms with average energies are determined for 700-800 eV projectiles for angles given above. The relation between the ion penetration depth and incidence angle is studied for both energy levels.

3. Results

Number of backscattered ions given in *figure 1* increased with increasing angles. The energy of backscattered particles is also recorded. For both 700 eV and 800 eV particles average energy of backscattered deuterium ions increased with the projectile angle. Backscattered ions hold more than 50% of the projectile energies.

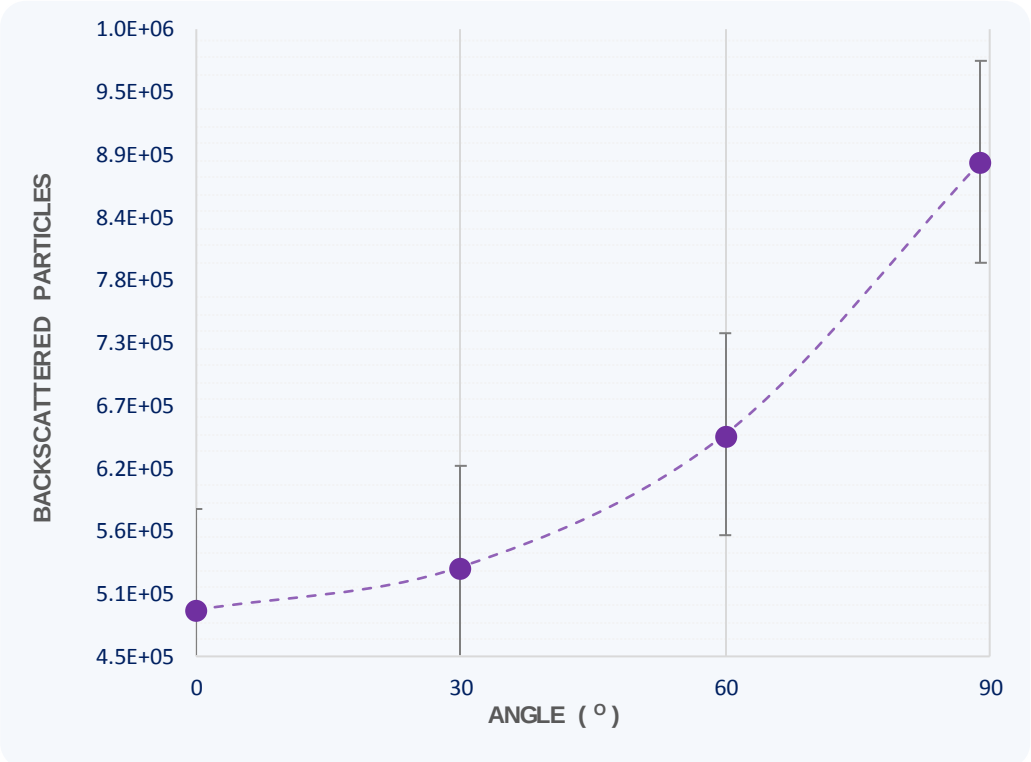

Figure 1. The number of the backscattered atoms for corresponding angles for 800 eV projectiles.

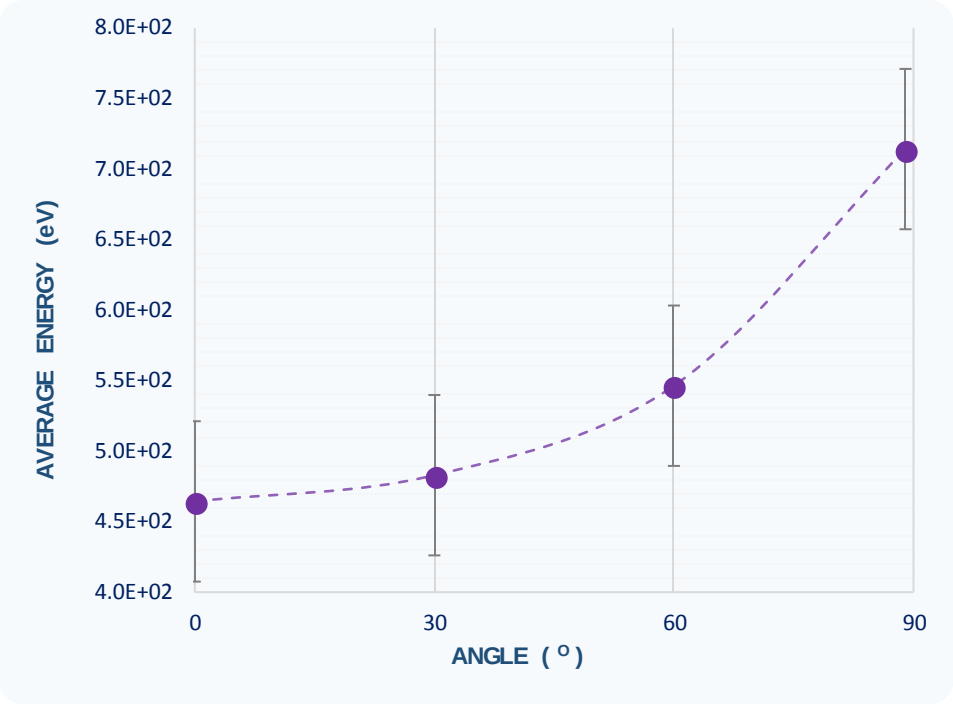

Figure 2. Average energy of backscattered particles for corresponding angles.

Among all backscattered particles, a considerable amount of the deuterium ions has energy values higher than 500 eV which will result in excavation due to secondary ions. To stay in the scope of this study only the backscattered particles with 700 eV and above are considered. The table below shows the energy distribution of backscattered 800 eV projectiles considering incidence angles from 0 ˚ to 89 ˚.

Backscattering Energy (eV)	**Total Ratio**
$E > 699$	34 %
$599 > E > 499$	20 %
$499 > E > 599$	14 %
$499 > E$	32 %

Table 1. Percent distribution of backscattered ion energies.

The proportion of backscattered ions with energy higher than 699 eV to all backscattered ions for the corresponding angle increased with incidence angle.

The rest of the ions are penetrated to the Tungsten layer. Implanted ions transfer their energy to atoms of the target surface and come to rest at a certain depth (Dearnaley, 1973 as cited in Behrisch & Eckstein, 2007). The value of the penetration depth is taken as the mean of all penetration values at the corresponding incidence angle. Depth values are higher for more energetic particles and inversely proportional to the projectile angle.

The surface binding energy of tungsten layer is taken as 8.68 eV as the default SRIM value. Number of excavated atoms per 1 million projectile and average energy per sputtered W atoms reached the maximum value at same projectile angle for both energy levels. As the incidence angle increased sputtering yield decreased continuously, on the other hand, the average energy of target atoms followed an irregular trend.

angle (°)	0,8 keV	0,7 keV
0	8,61	8,02
30	9,3	9,13
60	9,94	9,33
89	9,65	8,7

Table 2. Average energy per excavated atoms with corresponding angles.

angle (°)	0,8 keV	0,7 keV
0	0,007055	0,004048
30	0,007506	0,004588
60	0,008912	0,004789
89	0,003061	0,001309

Table 3. Sputtering yield with varying angles for 700 eV and 800 eV.

4. Discussion and Conclusions

In this study, the effects of H isotope bombardment on tungsten surface is investigated. Ion backscattering, excavation from the target surface, and penetration of H isotopes through the target are simulated with BCA. Angular dependency of such effects has been demonstrated.

SRIM calculations gave similar results for 700 eV and 800 eV projectile energies. For both energy levels sputtering yield and average energy per sputtered atom increased up to 55 degrees. The decrease in the sputtering yield of 800 eV projectile has been sharper than that of 700 eV at angles above 60^{o}. Detached tungsten atoms contaminate the plasma in the tokamak system, therefore tungsten atom sputtering should be well studied to maintain the plasma temperature at certain levels.

Higher energy and increasing projectile angle enlarged the number of the backscattered ions. Also, the average energy of backscattered ions has increased with incidence angle. For 800 eV projectiles, the portion of the backscattered ions with 699 eV and above energy increased at a positive rate. Backscattered ions with high enough energy would result in consecutive excavation from the target layer. Secondary effects of the backscattered ions require further studies considering the confinement theory.

References

B.D. Wirth, K. N. (2011). Fusion materials modeling: Challenges and opportunities. *MRS Bulletin*.

Behrisch, R., & Eckstein, W. (2007). *Sputtering by Particle Bombardment, Experiments and Computer Calculations from Threshold to MeV Energies.*

Chatzis, I., & Barbarino, M. (2021, May). *İnternational Atomic Energy Agency.* Retrieved July 29, 2021, from https://www.iaea.org/: https://www.iaea.org/fusion-energy/demonstration-fusion-plants

Hundur, Y., & Karateke, T. (2019). Investigation of Irradiation Mechanisms while Bombarding Fusion Reactor Wall with Deuterium.

Lasa, A., Schmid, K., & Nordlund, K. (2014). Modelling of W–Be mixed material sputtering under D irradiation. *Physica Scripta*(014059), 1-5.

Marian, J., Domain, C. S., Dudarev, S. L., Gilbert, M. R., Kurtz, R. J., Mason, D. R., . . . Sand, A. E. (2017). Recent advances in modeling and simulation of the exposure and response of tungsten to fusion energy conditions. *Nucl. Fusion, 57*(092008), 1-26.

Nordlund, K. H., Björkas, C., Ahlgren, T., Lasa, A., & San, A. E. (2014). Multiscale modelling of plasma–wall interactions in fusion reactor conditions. *Journal of Physics D: Applied Physics, 47*(224018).

Polvi, J., Heinola, K., & Nordlund, K. (2016). An interatomic potential for W–N interactions. *Modelling Simul. Mater. Sci. Eng., 24*(065007), 11.

Taniguchi, M., Sato, K., Ezato, K., Yokoyama, K., Dairaku, M., & Akiba, M. (2003). Sputtering of carbon–tungsten mixed materials by low energy deuterium,. *Journal of Nuclear Materials, 313–316*, 360-363.

Wampler, W., & Doerner, R. (2009). The influence of displacement damage on deuterium retention in tungsten exposed to plasma. *Nucl. Fusion, 49*(115023), 9.

International Conferences on Science and Technology
Natural Sciences and Technology
ICONST NST 2021

A New Perspective on Proteasome Inhibitors: A549 Lung Cancer Cell Microenvironment with M1 Polarized Macrophages

Selin Engür-Öztürk[1*], Elif Kaya-Tilki[2]

Abstract: Cell death and interactions between various components in the microenvironment are among the "hallmarks of cancer". Lung cancer is the leading cause of cancer-related deaths and today, the main goal of lung cancer research is to explore the molecular pathways of lung cancer pathogenesis, especially the specific mechanisms of tumor microenvironment. Also, proteasome inhibitors, bortezomib, and ixazomib are approved drugs for hematological malignancies, but lack anticancer activities study against most solid tumors. For this reason, we set up a model of THP-1 derived M1 macrophage polarization to mimic the communication between M1 macrophages and A549 lung cancer cells were co-cultured, with or without IC_{50} concentrations of bortezomib and ixazomib. After incubation, the effects of M1 polarized macrophages and proteasome inhibitors on A549 lung cancer cell apoptosis were evaluated morphologically and by mRNA gene panel expression levels. As a result, the co-culture of A549 cells with M1 polarized macrophage resulted in significant morphological changes in the cells. In addition, according to our RT-PCR results, it has been found that M1 polarized macrophage activates the proteasome pathway. Furthermore, bortezomib and ixazomib-induced cancer cell apoptosis-associated mRNA gene expression levels were significantly increased in cells co-cultured with M1 macrophages. These results suggest that M1 polarization may be a target of investigation of proteasome/immune-modulating therapies for lung cancer in the future.

Keywords: THP-1, macrophage, A549, bortezomib, ixazomib.

1. Introduction

Resistance to cell death, ability to escape immunological surveillance, triggered angiogenesis, interactions between various components in the microenvironment and others are the "hallmarks of cancer". Lung cancer is the leading cause of cancer-related deaths and today, the main goal of lung cancer research is to explore the molecular pathways of lung cancer pathogenesis, especially the specific mechanisms of tumor microenvironment (Denisenko et al., 2018; Siegel et al., 2019). Interaction with the microenvironment of cancer cells is primarily dependent on tumor-associated macrophages characterized as M1-and M2-polarized subtypes (Tsai et al., 2014). Proteasome inhibitors, bortezomib, and ixazomib are approved drugs for hematological malignancies, but lack anticancer activities against most solid tumors (Engür and Dikmen, 2017).
Studies have shown that M1 macrophages contribute to the suppression of tumor growth and increase the sensitivity of chemotherapy agents. However, the exact effects of M1

[1] Pamukkale University, Tavas Health Services Vocational School, Department of Pharmacy Services, Denizli, Turkey
[2] Anadolu University, Pharmacy Faculty, Department of Pharmacology, Eskişehir, Turkey
* Corresponding author: selino@pau.edu.tr

macrophages, on the regulation of proteasome- related gene expression and modulation of the biological behaviors of lung cancer cells apoptosis have not been fully elucidated. Here, we discovered the THP-1 derived M1 polarized macrophage' impacts on lung cancer cell A549 and proteasome inhibitors. We set up a model of macrophage polarization, starting from THP-1 monocytes differentiated into macrophages using PMA (Phorbol 12-myristate 13-acetate). Once differentiated (M0 macrophages), they were incubated with 20 ng/mL LPS plus IFN-γ in order to obtain M1 polarized macrophages. To mimic the communication between M1 macrophages and A549 cancer cells, they were co-cultured for 24 hours, with IC_{50} concentrations of bortezomib and ixazomib. Untreated A549 cells were used as control group. After the incubation, the impacts of M1 polarized macrophages and proteasome inhibitors on A549 lung cancer cell apoptosis were assessed by mRNA gene panel expression levels.

2. Materials and Methods

2.1. Cell culture and treatments

A549 non-small cell lung cancer (CCL-185, ATCC®, USA) and THP-1 human monocyte cell (TIB-202, ATCC®, USA) were cultured in 10% fetal bovine serum and 1% penicillin-streptomycin contained RPMI-1640 medium at 37°C in a humidified CO_2 incubator (Thermo Scientific™, USA), containing 5% CO_2. Cells were passaged at 70–80% intensity. Bortezomib (BioChemica, Germany) and ixazomib (Activebiochem, USA) were dissolved in DMSO and diluted to required concentrations with fresh medium. The control group was applied with medium containing 0.1% DMSO.

2.2. Polarization of macrophages into M1 subtypes

THP-1 cells were induced to differentiate into a macrophage-like phenotype by applying 100 ng/mL phorbol myristate acetate (PMA; Sigma, St Louis, MO) and were incubated serum-free medium for 24 hours. Differentiated, adherent cells were washed three times with culture medium (RPMI 1640 medium without PMA but containing 10% FBS and 1% penicillin-streptomycin) and rested for another 48 h in the culture medium to obtain the resting state of macrophages (M0). The attached cells, which corresponded to M0 macrophages, were polarized into M1 macrophages by adding 20 ng/mL LPS plus IFN-γ for 24 h. M1 polarized macrophages were extensively washed to eliminate carry-over cytokines and LPS incubated in fresh media for 24 hours. Macrophages have morphologically photographed with the Leica DM inverted light microscope.

2.3. Co-culture procedures

To study the effects of M1 polarized THP-1 macrophages on A549 cancer cell response to proteasome inhibitors bortezomib and ixazomib, M1 macrophages were cocultured with A549 lung cancer cells in indirect contact using Transwell (Corning, NY, USA) six-well plates inserts. The THP-1 monocytes were seeded into the upper chamber of the transwell apparatus, stimulated to differentiate into macrophages by the addition of 100 ng/mL PMA for 24 h, washed three times with phosphate-buffered saline (PBS), and incubated for another 48 h to eliminate the effect of PMA. The attached cells, which corresponded to M0 macrophages, were polarized into M1 macrophages by adding 20 ng/mL LPS plus IFN-γ for 24 h. A549 cells were seeded in the lower chamber 24 h before the end of macrophage polarization.
The upper chambers with the M1 macrophages were then placed directly on top of the six-well plates containing the A549 cells, and the two cell populations were incubated in the

presence of IC_{50} concentrations of bortezomib and ixazomib added directly into the wells for 24 h. Untreated A549 cells were used as control group. The effects of M1 polarized macrophages alone and in combination with proteasome inhibitors on A549 lung cancer cell morphology was photographed using Leica DM inverted light microscopy.

2.4. mRNA isolation and real-time polymerase chain reaction (RT-PCR)

The total RNA isolated from the A549 lung cancer cells to single-cell control, and the co-cultured lung cancer cells and M1 macrophages treated with bortezomib or ixazomib to determine the change in genes in the apoptosis pathway, were extracted using a MagNA Pure Compact RNA Isolation Kit for the MagNA Pure Compact Instrument LC 2.0 system (Roche Diagnostics, Mannheim, Germany). The total mRNA amounts of the samples were measured at 260 and 280 nm in the NanoDrop 2000® (Thermo Fisher, USA) spectrophotometer. cDNA was obtained using the Transcriptor High Fidelity cDNA Synthesis Kit® (Catalog no: 05091284001, Roche, Germany) following the kit protocol from 100 ng/µl mRNA of each sample. After the cDNA samples were replicated by PCR method, the expression levels were determined with the Light Cycler® 480 Real-Time PCR System (Roche, Germany) using the Realtime-ready Custom Panel 96/24+ (Config. No: 100024087, Roche, Germany) containing the gene responsible for proteasome and apoptosis pathway. Glyceraldehyde 3-phosphate dehydrogenase (GAPDH) was used was used as housekeeping gene. Results were analyzed according to the changes in the amplification levels compared to the A549 control group with the analysis software of the instrument.

3. Results

3.1. M1 macrophage polarization

THP-1 cells were applied to 100 ng/mL PMA concentration for 24 hours and the attached cells, which corresponded to M0 macrophages, were polarized into M1 macrophages by adding 20 ng/mL LPS plus IFN-γ for 24 h. Macrophage cells were photographed with Leica DM 300 Inverted microscope (**Figure 1**).

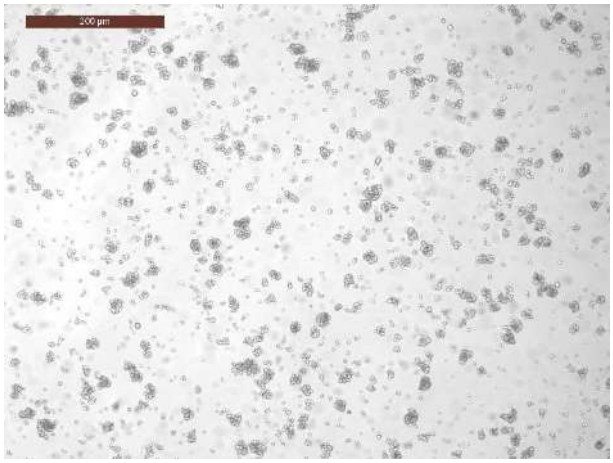

THP-1

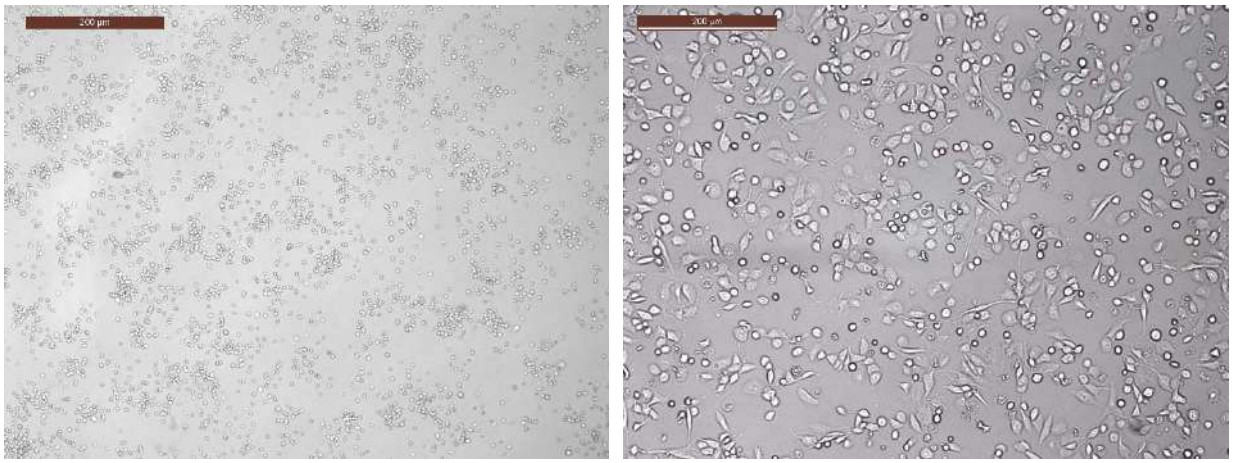

M0 **M1**

Figure 1. Microscope image of THP-1, THP-1 derived macrophage (M0) and M1 polarized macrophage (10X)

3.2. Determination of A549 lung cancer cell morphology in M1 macrophage co-culture

In this study, we found that exposure A549 cells to M1 macrophage can cause morphological changes. Initially, A549 cells have a typical cuboid epithelial morphology with tight cell-to-cell contacts, according to the control group. The co-culture of A549 cells with M1 polarized macrophage for 24 hours resulted in significant changes in cell morphology. The cells' morphology changed from cuboid to spindle-shaped or fibroblast-like, and cell-to-cell contacts became less intense. Furthermore, A549 cell viability was reduced and apoptotic bubble was observed in the bortezomib or ixazomib co-culture groups with M1 macrophage (**Figure 2**).

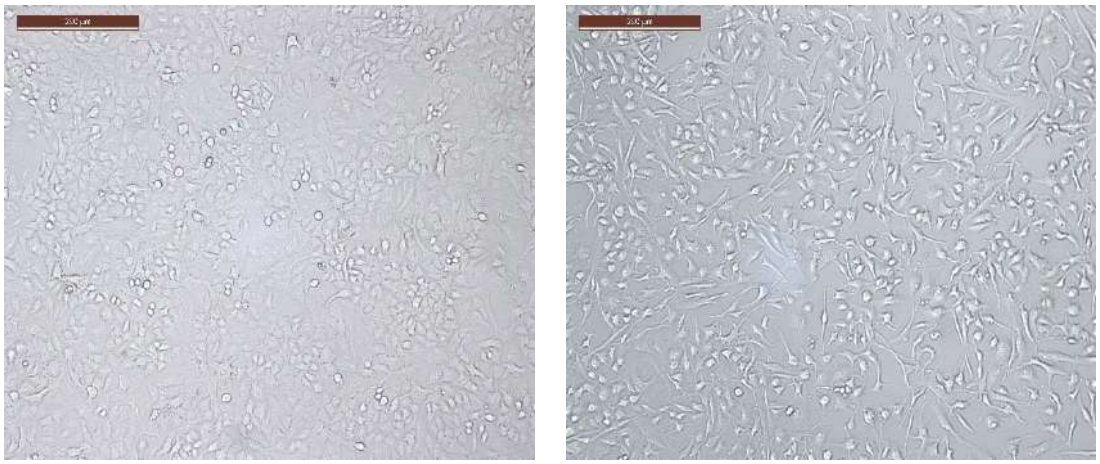

A549 Control **A549 + M1 Macrophage**

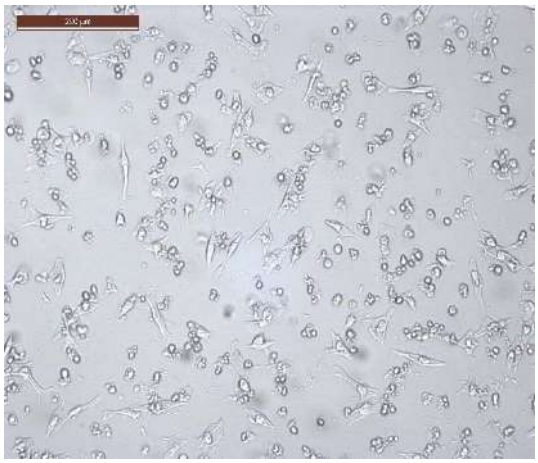

A549+M1 Bortezomib

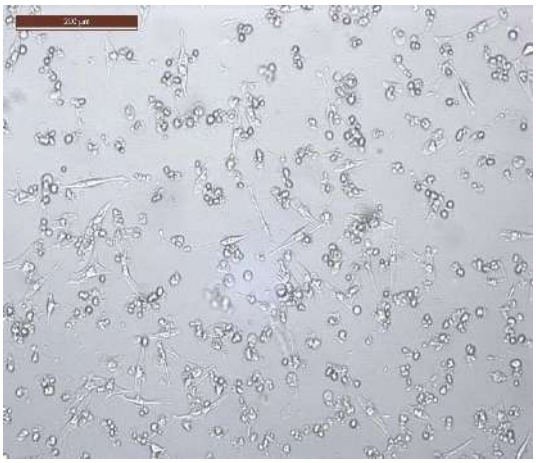

A549+M1 Ixazomib

Figure 2. Morphological changes in A549 cells.

3.2. Determination of the gene expression levels of apoptosis and proteasome pathway

According to our RT-PCR results, it has been found that M1 polarized macrophage activates the proteasome pathway mediated by NFkB1, NFkB2, NFkBIA and NFkBIB genes. Ixazomib, specifically bortezomib, may have inhibited the proteasome pathway activated by M1 macrophages in A549 cells, as evidenced by a decrease in NFKB1 and NFkBIA mRNA expression. Upregulation of the proapoptotic Bcl-2 family of proteins, such as BAX, BID, and BAK1, triggers apoptosis (You et al., 2017). According to our results, A549 cell apoptosis may have been induced as a result of increased mRNA expression in the BAX gene with bortezomib and in the BID gene with ixazomib. According to our results, it was determined that when M1 macrophage was used alone or with bortezomib or ixazomib, it significantly increased Casp9 mRNA expression levels and induced apoptosis pathway (**Table 1**).

Table 1. mRNA expression levels fold changes in proteasome inhibition pathway-related genes

Gene Name	**Gene Symbol**	**Fold Changes**			
		A549 Control	**A549+M1**	**A549+M1 Bortezomib**	**A549+M1 Ixazomib**
Nuclear factor kappa B subunit 1	NFkB1	1.00	2.247	0.5249	1.317
Nuclear factor kappa B subunit 2	NFkB2	1	2.289	2.105	4.640
NFkB inhibitor alpha (IkBA)	NFkBIA	1	2.272	0.5376	0.7579
NFkB inhibitor beta (IkBB)	NFkBIB	1	1.307	1.548	3.546
RELB proto-oncogene, NFkB subunit	RELB	1	1.406	1.146	1.878
Interleukin 6	IL-6	1	5.180	5.754	8.248
Interleukin 8	IL-8	1	0.9540	2.043	1.678
Tumor protein p53	TP53	1	0.6239	0.0435	0.0644
Breakpoint cluster region	BCR	1	0.9802	65.05	4.737
phosphoinositide-3-kinase, catalytic,	PIK3CA	1	1.574	2.419	2.672

alpha polypeptide					
BCL2 antagonist/killer 1	BAK1	1	0.2445	0.3905	0.00168
BCL2-associated X protein	BAX	1	0.1047	7.713	0.0485
BCL2-like 1	BCL2L1	1	0.2017	0.3840	0.5098
BH3 interacting domain death agonist	BID	1	0.3529	0.4486	1.745
Caspase 7	CASP7	1	0.5715	0.6826	0.0863
Caspase 9	CASP9	1	2.777	17.56	24.20
FA complementation group D2	FANCD2	1	0.2290	0.1596	0.0281

4. Discussion and Conclusions

The initiation and metastasis of lung cancers depend not only on the genetic and molecular characteristics of the cancer cells but also on their interaction with the immune system and the microenvironment of the tumor (Forde et al., 2014). Macrophages can be differentiated into M1 or M2 macrophages depending on the stimulus in their environment and recent studies suggest that macrophage polarization could serve as anti-cancer and anti-angiogenic therapeutic strategies (Yuan et al., 2015). Studies have shown that M1 macrophages contribute to the suppression of tumor growth and increase the sensitivity of chemotherapy agents (Genin et al., 2015; Yuan et al., 2015). In our study, it was found that M1 macrophages had an effected alone and increased the bortezomib and ixazomib-induced apoptosis. Therefore, in this study, we further demonstrated that macrophages with M1 polarizations differentially affect proteasome inhibitor pathway and apoptosis gene expression profiles of lung cancer cells. In conclusion, because all new directions for drug development are based on a broad knowledge of the microenvironment of the tumor, understanding the mechanisms that modulate the microenvironment of the tumor may facilitate the development of novel anticancer therapy and may lead to greater success in the eradication of lung cancer. These results suggest that M1 polarization may be a target of investigation of proteasome/immune-modulating therapies for lung cancer in the future.

References

Bragança, H., Diogo, E., Moniz, F., Amaro, P., (2009). First report of pitch canker on pines caused by Fusarium circinatum in Portugal. Plant Disease, 93(10), 1079-1079.

Denisenko, T. V., Budkevich, I. N., Zhivotovsky, B., (2018). Cell death-based treatment of lung adenocarcinoma. Cell death & disease, 9(2), 117.

Engür, S., Dikmen, M., (2017). The evaluation of the anti-cancer activity of ixazomib on Caco2 colon solid tumor cells, comparison with bortezomib. Acta clinica Belgica, 72(6), 391–398.

Forde, P. M., Kelly, R. J., Brahmer, J. R., (2014). New strategies in lung cancer: translating immunotherapy into clinical practice. Clinical cancer research: an official journal of the American Association for Cancer Research, 20(5), 1067–1073.

Genin, M., Clement, F., Fattaccioli, A., Raes, M., & Michiels, C., (2015). M1 and M2 macrophages derived from THP-1 cells differentially modulate the response of cancer cells to etoposide. BMC cancer, 15, 577.

Siegel, R. L., Miller, K. D., & Jemal, A., (2019). Cancer statistics, 2019. CA: a cancer journal for clinicians, 69(1), 7–34.

Tsai, M. J., Chang, W. A., Huang, M. S., Kuo, P. L., (2014). Tumor microenvironment: a new treatment target for cancer. ISRN biochemistry, 2014, 351959.

You, Y., Cheng, AC., Wang, MS. et al., (2017). The suppression of apoptosis by α-herpesvirus. Cell Death Dis 8, e2749.

Yuan, A., Hsiao, Y. J., Chen, H. Y., Chen, H. W., Ho, C. C., Chen, Y. Y., Liu, Y. C., Hong, T. H., Yu, S. L., Chen, J. J., & Yang, P. C., (2015). Opposite Effects of M1 and M2 Macrophage Subtypes on Lung Cancer Progression. Scientific reports, 5, 14273.

International Conferences on Science and Technology
Natural Sciences and Technology
ICONST NST 2021

Variation of Mean Free Path for Collision 'O+ + N2' During The Solar Eclipse

Mehmet Yaşar[1*]

Abstract: The sun is one of the most effective parameters in forming the Earth's ionosphere. Therefore, the study of solar-induced events will greatly contribute to the understanding of ionosphere uncertainties. The solar eclipses are important events that cause sudden and medium-scale disturbances in the earth's ionosphere. In addition to electromagnetic wave propagation, there are also perturbations in ionosphere chemistry during and after the eclipse. In this study, the mean free path for the 'O+ + N2' collision during the eclipse was investigated depending on the altitude and local time parameters. The obtained results showed that the mean free path started to decrease from sunrise and then reached its lowest value at the maximum coverage time.

Keywords: Solar eclipse, Ionosphere, Ionospheric collision processes.

1. Introduction

The ionosphere structures are degenerated due to solar eclipse, and many researchers have conducted different models, theories and observations researches on the ionospheric response to solar eclipse. In order to investigate the effect of solar on the ionosphere, several theoretical models on the behaviour of the atmosphere during the solar eclipse were developed. Further, observation and investigation of ionospheric structure during solar eclipse have contributed extremely to the understanding transport, dissociation, recombination, diffusion, collisions, production and loss processes as well as radio propagation. The description of the photo-chemical processes and the ionosphere chemical kinetics in the theoretical model, with the account of chemical composition of the neutral particles and ions considered, includes the processes of photo-ionization, photo-dissociation, dissociative recombination, radiative recombination, collision mechanism, etc. One of the most important reactions involving the loss of O+ in the ionosphere is 'O+ + N2' collision processes.

2. Methodology

Several statistical quantities such as the mean free path, collision frequency and total number of reactive collisions must be taken in to account and so shall find quantitative relationships between statistical quantities characterizing molecular collisions (such as mean free path, etc.) and basic physical properties of the gas (such as con¬centration, temperature, height, etc.).

[1] Firat University, Science Faculty, Department of Physics, Elazığ/TURKEY
* Corresponding author: mehmetyasar@firat.edu.tr

2.1. Mean free path model

The free path is the distance traveled by a molecule between two consecutive colli¬sions. The mean free path is the average distance between two consecutive collisions of a single molecule.

$$\lambda = 1/\sigma N \quad (1)$$

Where σ and N are reaction cross section and density.

3. Results and Discussion

In this study, the mean free path values for the 'O+ + N2' collision were calculated for the ionospheric height (187.3 km) and local time (LT) during the solar eclipse (March 29, 2006). The N2 density change with local time at 187 km is given in Fig. 1.

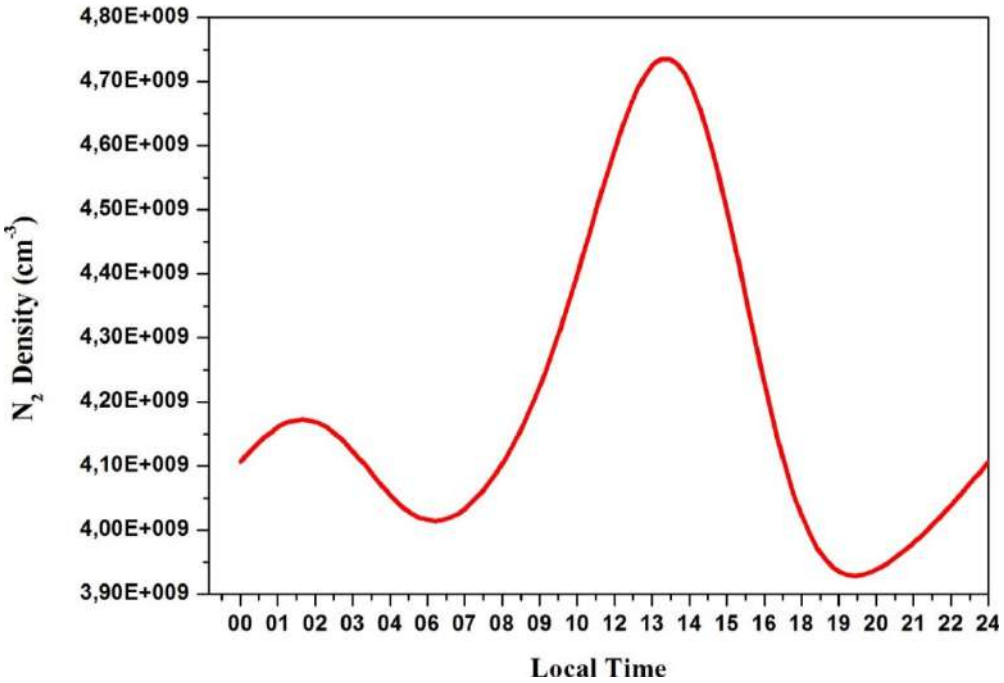

Figure 1. Change of N2 Density with time.

As can be seen from Fig. 1, the N2 density reaches maximum value around LT 13:30. In this study, neutral densities (N2) were taken from the NRLMSIS-00 atmospheric model. Since this model is a semi empirical model, we cannot fully observe the eclipse effect in Fig. 1.
The mean free path change with local time at 187 km is given in Fig. 2.

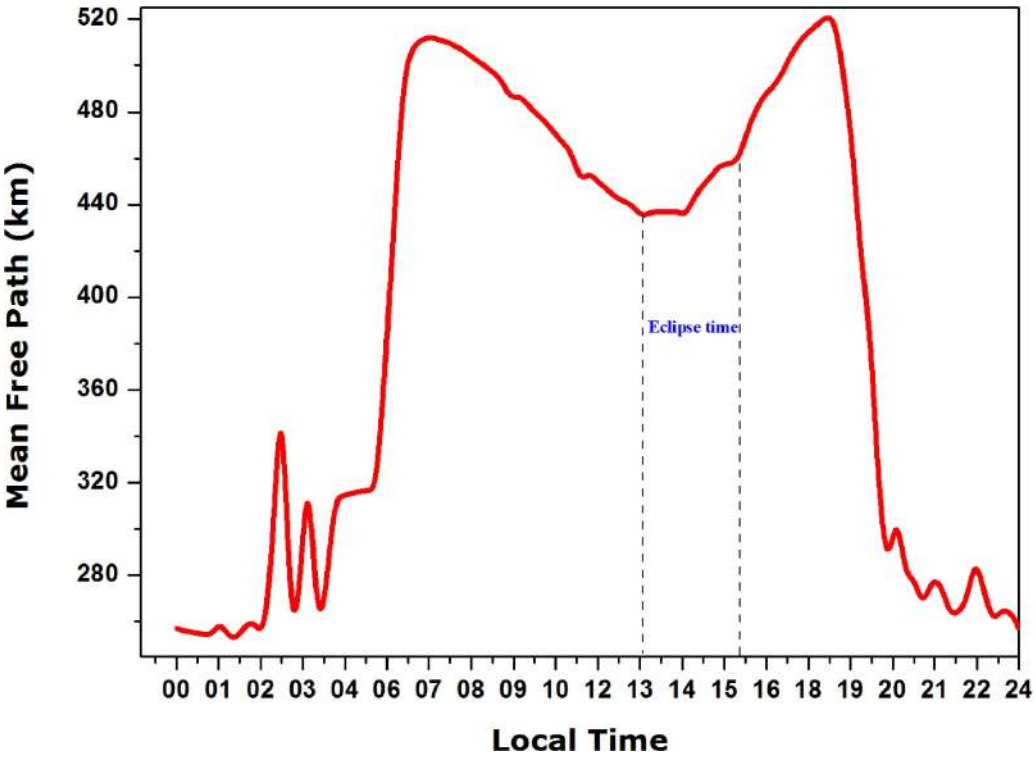

Figure 2. Change of mean free path with time.

As can be seen from Fig. 2, the mean free path took its minimum value during the eclipse time.

The mean free path showed a steady decreasing trend from the beginning of the eclipse to the maximum covered and then started to increase. Although the lowest value of the mean free path during the eclipse was expected to occur at the time of maximum covered, this value was seen between partial eclipse and maximum covered. This is because the mean free path varies depending on both the neutral density and cross section. As can be seen from Eq. 1, the mean free path varies inversely with the cross section and the neutral density. The neutral densities were taken from the NRLMSIS-00 atmospheric model, which made semi-experimental measurements, while the cross section was calculated according to the measurement values which are taken from the Kharkov incoherent scatter radar.

Therefore, it is clear that the calculations to be made with the data obtained from the radar stations will give more consistent results in the evaluation of the solar eclipse effect where sudden changes occur on the ionosphere.

4. Conclusion

The following results were obtained in this study, which investigated the mean free path variation for the 'O+ + N2' collision during the solar eclipse.

The mean free path increased from maximum covered to the end of the partial eclipse.

The mean free path took the lowest value in the daytime between the onset of the eclipse and the maximum covered.

The mean free path reached the maximum value at the time after the eclipse.

The maximum value of N2 density was seen at 13:30 for local time.

The effect of solar eclipse on N2 density did not observed.

Acknowledgments

The author thanks the Community Coordinated Modelling Center for the NRLMSISE-00 atmosphere model for neutral density data, and directors of Kharkov IS Radar.

References

[1] Chernogora L F, Domnin I F, Emelyanov L Y and LyashenkoMV2019 Physical processes in the ionosphere during the solar eclipse on March 20, 2015 over kharkiv, Ukraine (49.6° N, 36.3° E) J. Atmos. Sol. Terr. Phys. 182 1

[2] Sağir S., Yaşar M., Atici R. 2019. The Relationship between Dst, IMF-Bz and Collision Parameters for O+ + N2 → NO+ + N Reactive Scattering in the Ionosphere. Geomagnetism and Aeronomy, 59 (8): 1003-1008.

[3] Yaşar M. 2021. The Change of Diffusion Processes for O+ + N2→NO+ + N Reaction in the Ionospheric F Region During the Solar Eclipse Over Kharkov. Thermal Science, 25 (1): S51-S56.

[4] Yaşar M. 2021. Investigation of ionospheric losses for the 'O++O2 → O2+ + O' reaction during the solar eclipse. Physica Scripta, 96.

[5] https://ccmc.gsfc.nasa.gov/modelweb/models/nrlmsise00.php

[6] Gombosi T I 2003 Gaskinetic Theory (New York: Cambridge University Press)

[7] Chernogora L F, Domnin I F, Emelyanov L Y and LyashenkoMV2019 Physical processes in the ionosphere during the solar eclipse on

March 20, 2015 over kharkiv, Ukraine (49.6° N, 36.3° E) J. Atmos. Sol. Terr. Phys. 182 1

International Conferences on Science and Technology
Natural Sciences and Technology
ICONST NST 2021

Marketing Research on Consumer Behavior When Buying Bottled Water

Sofija Thompson[1*]

Abstract: Water is one of the most important resources on the planet. The use and consumption of bottled water has become a significant phenomenon in recent decades. The number of bottled water brands on the market are increasing, and bottled water is increasingly being advertised as a healthy lifestyle and a symbol of prestige and status. Consumption of bottled water has also increased in Serbia, where bottled water used to be bought and used only on special occasions. Nowadays, companies often face challenges related to interaction with consumers and the main priority is the consumer experience. Before offering them new products, companies must know what the consumer needs, how they think and what their questions are. Therefore, marketing research requires a constant flow of information. To create a quality marketing plan, it is necessary to know the market, customers, consumers, and competitive activities. Market research largely provides support to managers in making decisions, and it represents an already designed process of data collection as well as analysis.

The aim of this paper is to examine the extent to which consumers in Serbia buy bottled water, whether they trust companies that sell branded products or the city's water supply system more. In addition, how much influence good marketing has on consumers in product placement.

Data collection for this survey was conducted by an online survey by sending questionnaires to e-mail addresses of consumers in Serbia. The paper will present the results conducted on a sample of at least 200 respondents of all ages.

Keywords: Marketing research, consumers, bottled water, product branding

1. Introduction

Bottling of water is a profitable branch of industry, and profitability has led to a large number of producers, which has created great competition in the market. In Serbia, the quality and properties of bottled water are regulated by the Ordinance on the hygienic quality of drinking water (Pravilnik o kvalitetu i drugim zahtevima za prirodnu mineralnu vodu, prirodnu izvorsku i stonu vodu), as well as the Ordinance on quality and other requirements for natural mineral, natural spring and table water (Pravilnik o higijesnkoj ipravnosti vode za piće) for natural mineral water, natural spring and table water. The reasons for consuming it are different and usually start from the belief that this water is healthier than tap water (Paunović, 2020). The supply of water from the public water supply system speaks of someone taking care of us instead of us and taking all the necessary steps to free the water from unwanted microorganisms and to reach the user in a healthy condition. Due to environmental pollution

[1] University of Belgrade, Faculty of organizational sciences, Belgrade, Serbia
*Corresponding author: sofijathompson78@gmail.com

from non-degradable or recyclable packaging, the European Union has expressed the view that its members must take the necessary steps to reduce the use of bottled water and to increase confidence citizens into the tap water. In the time of globalization and intense competition in business, companies are increasingly focused on long-term relationships with consumers, so the key activity of companies is marketing (Borisavljević, 2013). Marketing research is a weapon used to listen to consumers (Gates, 1999, str. 187-189).
Companies need to understand what the consumer needs and how consumers think in order to be able to offer improved or new products (Prokopović, 2007, str. 16-29).

A survey on consumer behavior when buying bottled water was conducted in June 2021 through an online survey in which 20 closed questions were asked. 200 respondents from all over Serbia participated in the research. The main goal of this paper is to theoretically and methodologically show the impact of marketing on consumer behavior when buying bottled water.

In addition to the introduction, the paper contains four more works. The second part explains the methodological approach of the research, while the third part describes a review of the literature that indicates the development and importance of marketing relationships and consumer loyalty. The fourth part presents the results of the research and indicates the influence of marketing on consumer behavior. The last part of the paper contains a discussion and a conclusion.

2. Metodology

The collection of basic data for the research was done through an online survey conducted by sending questionnaires to e-mail addresses, viber and social networks (LinkedIn, Facebook). The survey consisted of 20 closed questions related to bottled water consumption. Respondents were of all ages throughout Serbia. The following methods were used during the research:

- Research of primary and secondary material,
- Analytical and synthetic method,
- Comparative and descriptive method.

The basic research process is the analysis of secondary material, which included the processing of domestic and foreign literature in the field of marketing and consumer loyalty.

3. Literature review

According to Peter Drucker, the basic idea for the company's success is marketing, development and research, because these functions create value. Drucker argues that other functions only produce (Drucker, 1993). From a historical perspective, relationship marketing is not a new invention. Before the Industrial Revolution and before mass production, businesses were oriented toward personal services and direct contact with store owners who cared for and met the needs of individual customers (Peppers & Rogers, 1995). When mass production began, companies focused on selling their products and services. Long-term orientation is crucial if a firm intends to try to change the global market (Kandampully & Duddy, 1999, str. 317-318).

According to Gronroos (Grönroos, 1994, b.) Relationship marketing was first introduced by Berry in terms of marketing services. Christoper et al. (Christopher , Payne, & Ballantyne, 1991) propose the integration of customer service, quality, and marketing through marketing

relationships. They are of the opinion that relationship marketing will help a company focus on customer retention, follow a long-term vision, emphasize customer service, produce customer commitment, and ensure quality (Kandampully & Duddy, 1999, str. 319). The development and importance of marketing relationships towards Buttle (Buttle, 1996), Peppers and Rogers (Peppers & Rogers, 1995) and Bitner (Bitner, 1995) are increasingly intense competition and increasingly demanding and sophisticated customers.

Berry (Berry, 1982) argues that a company's success in a highly competitive market depends on its ability to retain a customer base. The strategic advantage of the company is in maintaining the customer base, as opposed to focusing only on attracting new ones. Customer retention is less expensive than acquisition (Heskett, Sasser, & Hart, 1990).
When it comes to consumer loyalty, it can be defined as a consumer's commitment to a particular brand or business entity. If the consumer has a pronounced attitude and behavior towards the purchase of a certain product, it is clear that he is a loyal consumer (Marinković, 2012). Loyalty is recognized as a very valuable assessment in a competitive market (Srivastava, Shervani, & Fahey, 1998). In service marketing, loyalty can be viewed in two ways (Gwinner, Gremler, & Bitner, 1998).

According to the first, loyalty is seen as a repetition of consumer behavior in the purchase of a particular service, while the second approach views loyalty in terms of repeating their behavior and their positive attitude. Over the past decade, customer loyalty has prevailed in several industries (Herschell, 1997). Membership in various loyalty programs is also very popular among consumers (Libermann, 1999). This has led to increased competition from different companies within the same industry, which compete to cater to the same group of consumers (Passingham, 1998).

3.1. Marketing channels

According to Kotler and Keller, marketing management is the science and skill of choosing the right markets, as well as attracting customers, retaining them and expanding the customer base, which is why it is very important to choose the right channels through which messages are sent (Kotler & Keller, 2009, str. 15). An important part of marketing theory is internet marketing, because marketing goals are achieved through the application of digital technology. The Internet has changed many marketing customs and introduced most companies to network marketing (Lovreta , Končar, & Petković, 2011, str. 8-9). On the Internet, marketing activities can be applied as a form of communication between product manufacturers and their customers.

There is a difference between the terms brand and branding, which is reflected in the fact that the brand is created by persistent and long-term work with careful planning and long-term investment. Branding is a process that involves the implementation of a marketing program to build brand value (Bolfek, Jakičić, & Lončarić, 2012). In overcoming market disparities, the role of marketing channels creates better value for consumers in the personal consumption market at the lowest cost (Juttner, Christopher, & Baker, 2006).

4. Research analysis

The sample on which the research was conducted consists of 200 respondents, 49.55% male and 50.45% female. The largest number of respondents belongs to the age group of 35-44 years, 30.63%, and from 45-54 years, 22.97%. By regions, 24% of respondents are from Belgrade, 27% from Vojvodina, 27% from eastern and southern Serbia, and 22% from western Serbia and Sumadija. The aim of the research is to examine the extent to which the inhabitants of the Republic of Serbia use bottled water.

Figure 1 shows the results showing the use of bottled water. Based on the obtained results, it can be seen that 64% of citizens drink bottled water, and only 17% drink exclusively tap water. By regions, the largest percentage of bottled water is consumed by the inhabitants of Vojvodina, 79.6%, which is expected considering the quality of water in that part of Serbia. Only 1.5% of respondents would consume bottled water, but cannot afford the additional cost, while 5.5% avoid buying bottled water because they believe that plastic packaging is harmful to the environment.

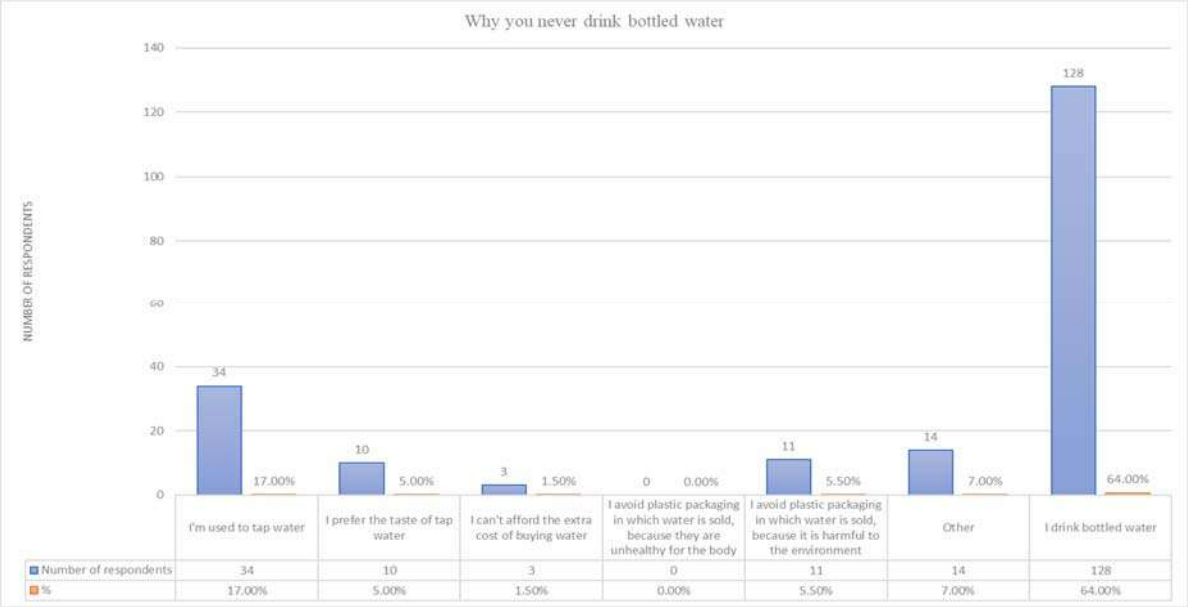

Figure 1. Why you never drink bottled water

In the choice of the bottled water brand, two manufacturers stood out in the leading position, as shown in Figure 2. The "Rosa" brand is consumed by 51.4% of respondents, while "Aqua Viva" is consumed by 50.8% of respondents. The least popular brand is water "Jazak" and it is consumed by 2.7% of citizens, which was expected considering the region of Vojvodina where water is produced. After Rose and Aqua Viva, the brand "Voda voda" stands out with 18.9%, followed by "Mg Mivela" with 15.7%, then "Jana" with 9.7% and "Voda Vrnjci" with 7, 6%.

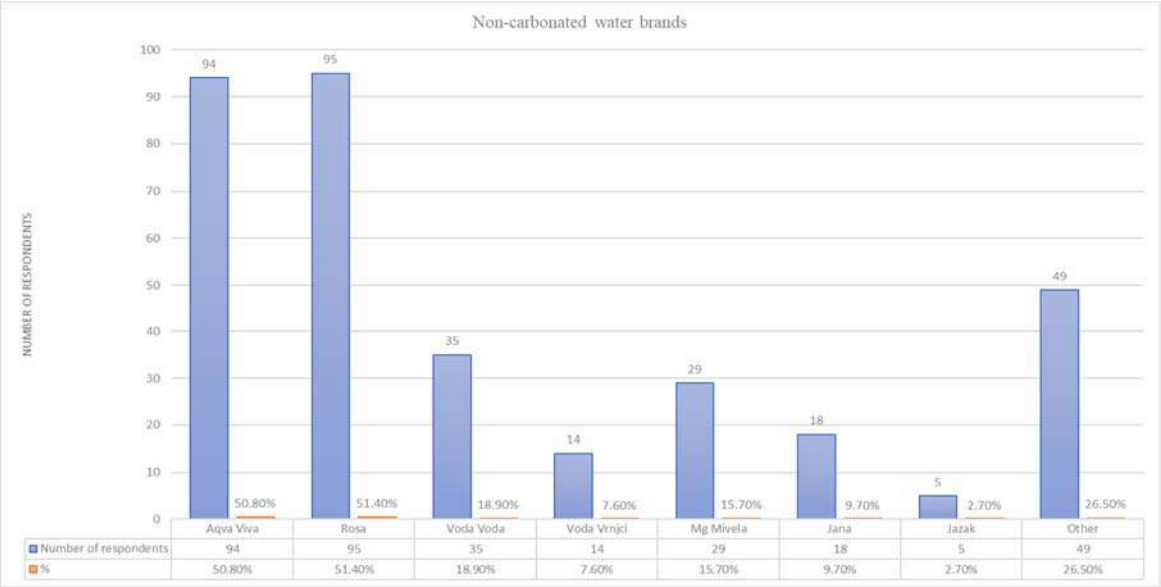

Figure 2. Non-carbonated water brands

The reasons for choosing the brand of bottled non-carbonated water among the respondents are shown in Figure 3, and the largest percentage of respondents like the taste of water, 48.1%, while 41.6% of them believe that it is a quality product. Only 13.5% opt for a certain brand because of the price, and 21.6% have created a habit towards a certain manufacturer. The combination of minerals is important for 7.6% of respondents, while 8.6% pay attention to the appearance of the packaging. Product availability gained the trust of 17.3% of respondents.

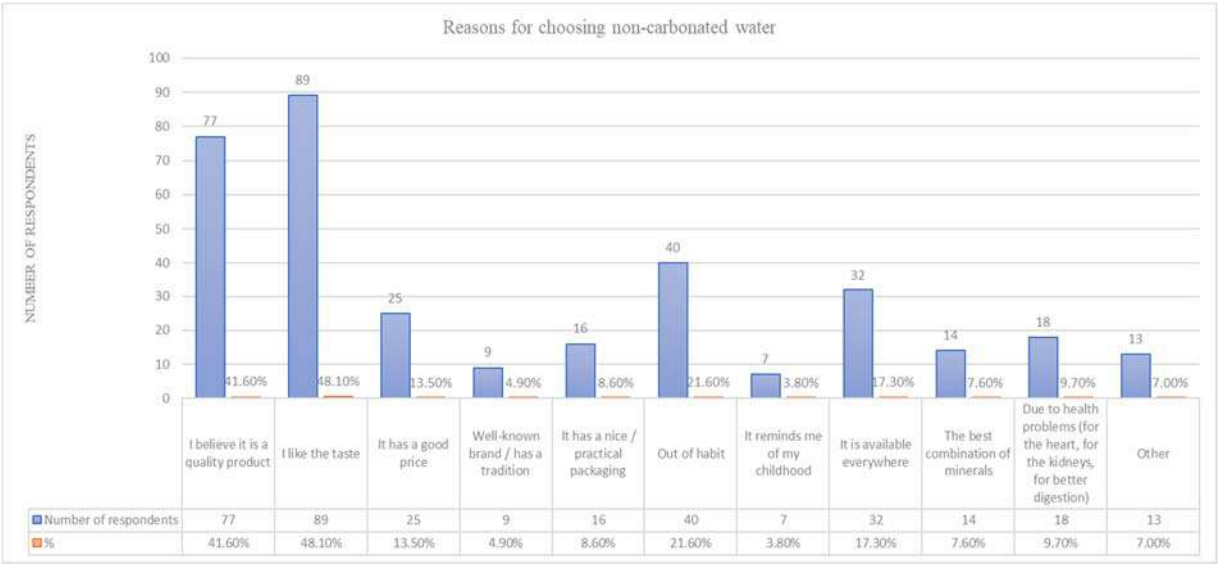

Figure 3. Reasons for choosing non-carbonated water

Consumers are mostly determinated for the use of bottled water while walking, 50% of respondents, while 47.7% consume it in restaurants and cafes. When it comes to carbonated water, 34.9% consume it with food for digestion, and 9.9% with alcoholic beverages. Carbonated water is consumed daily by 9.5%, two or three times a week by 20.5%, while 23.5% of respondents consume several times a month or several times a year.

The research shows that flavored water is not very popular on the territory of Serbia because 61% of respondents have never consumed it. Only 1.5% consume it once a week, and 55.5% buy it once a year.

When it comes to water intake during the day, 25% of respondents drink 2 liters of water per day, while 1% drink only two glasses of water during the day. The majority of respondents, 58%, are satisfied with the water intake, while only 6.5% say that it does not matter to them. 1.5% use the application as a reminder for water consumption, while 43.5% of respondents do not use it at all, but they think it is a good idea. The largest number of respondents, 55%, do not use applications and do not intend to use them.

The most popular bottled water packaging is 0.5liter bottles and 46.5% of respondents buy it. 1.5liter bottles are in second place and 38% of respondents buy them. 2.5-liter bottles and 5-liter balloons are less popular because only 3% of respondents buy them.
The obtained results can greatly help companies in planning the production and sale of water, as well as in planning a strategy for competitive advantage, understanding the wishes of customers and creating an appropriate image.

5. Conclusion

Marketing activities greatly influence product placement, and product quality makes consumers loyal to a particular brand. In order for companies to build the concept of loyalty, they must make their service quality. Modern marketing practice indicates that consumer enthusiasm for a certain product is needed, and not just its satisfaction. When the consumer is very satisfied with the product, he becomes its main promoter. The results of the research show that the price of the product does not affect consumer loyalty, but the quality and taste of the product. Taking the price into account, it can be concluded that public companies, whose activity is the production of safe and quality drinking water, do not invest enough funds in marketing as companies that produce bottled water do. Drinking water from the tap has a significantly lower price than bottled water, 0.059 dinars per liter of water, while a liter of bottled water averages 50 dinars. By setting a noticeable difference between products through branding and franchise development of loyal customers, marketers create value that can be translated into financial gain for the company. Marketing indicators reflect the condition and position of a brand respected from the aspect of its final result, which means from the aspect of consumers, because business success is conditioned more by consumers, and much less by producers.

Based on the conducted research, it is concluded that bottled water producers can significantly improve and enhance their business by obtaining useful information on how customers evaluate the quality of services, and based on that identify factors that generate loyalty to increase their competitiveness. advantage and profit in the long run.

6. References

Berry, L. (1982). *"Relationship marketing", in Berry, L.L., Shostack, G.L.,Upah, G.D. (Eds), Emerging Perspectives on Services Marketing, AMA Services Marketing.* Chicago, IL: American Marketing Association.

Bitner, M. (1995). "Building service relationships: its all about promises". *Journal of the Academy of Marketing Science, (23)*, 4: 246-251.

Bolfek, B., Jakičić, D., & Lončarić, B. (2012). *Polazišta za brendiranje Slavonije kao turističke destinacije.* Ekonomski vjesnik No.2.

Borisavljević, K. (2013). *Relationship Marketing: Exploring relational strategies in Marketing.* Kragujevac: Ekonomski horizonti.

Buttle, F. (1996). *Relationship Marketing – Theory and Practice.* London: Chapman.

Christopher , M., Payne, A., & Ballantyne, D. (1991). Relationship Marketing. *Oxford: Butterworth-Heinemann*.

Drucker, P. (1993). *Management: Tasks, Responsibilities, Practices.* Harper Collins.

Filipović, V., & Janičić, R. (2010). *Strateški marketing.* Beograd: Fakultet organizacionih nauka.

Gates, B. (1999). *Business @ the speed of thought.* New York: Warner Books.

Grönroos, C. (1994, b.). . „From Marketing Mix to Relationship Marketing:Towards a Paradigm Shift in Marketing". *Management Decision, (32)*, 4-20.

Gwinner, K., Gremler, D., & Bitner, M. (1998). Relational Benefits in Services Industries: The Customer's Perspective. *Journal of the Academy of Marketing Science, 26(2), 101–114. doi:10.1177/0092070398262002.*

Herschell, L. (1997). Does your "loyalty" program inspire any loyalty. *Direct Marketing*, 46-48.

Heskett, J., Sasser, W., & Hart, C. (1990). *Service Breakthroughs.* Free Press.

Juttner, U., Christopher, M., & Baker, S. (2006). *Demand chain management-integrating marketing and supply chain management.* Industrial Marketing Management Vol.36, No.3, pp.377-392.

Kandampully, J., & Duddy, R. (1999). „Relationhsip marketing: a concept beyond the primary relationship". *Marketing Intelligence & Planning (17)*, 315-323.

Kotler, P., & Keller, K. (2009). *Marketing Management.* New Jersey: Pearson/Prentice Hall.

Libermann, Y. (1999). Membership Clubs as a Tool for Enhancing Buyers' Patronage. *Journal of Business Research, 45(3) doi:10.1016/s0148-2963(97)00241-5.*, 291-297.

Lovreta , S., Končar, J., & Petković, G. (2011). *Strategije izgradnje strukture kanala marketinga u funkciji jačanja konkurentnosti srpske privrede.* Beograd: Ekonomski fakultet.

Marinković, V. (2012). *Marketinški aspekti satisfakcije i lojalnosti.* Kragujevac: Ekonomski fakultet.

Passingham, J. (1998). Grocery retailing and the loyalty card. *Journal of Market Research Society*, 55-63.

Paunović, K. (2020, Januar 27). Flaširane vode-za i protiv. Beograd.

Peppers, D., & Rogers, M. (1995). „A new marketing paradigm: share of customer, not market share". *Planning Review, 2*, 14-18.

Pravilnik o higijesnkoj ipravnosti vode za piće. (n.d.). Sl. list SRJ, br. 42/98 i 44/99 i Sl. glasnik RS, br. 28/2019.

Pravilnik o kvalitetu i drugim zahtevima za prirodnu mineralnu vodu, prirodnu izvorsku i stonu vodu. (n.d.). Službeni list SCG 53/2005, Sl. glasnik RS, 43/2013.

Prokopović, B. (2007). *Osnovi marketinga (7. izdanje).* Beograd: Proinkom.

Srivastava, R., Shervani, T., & Fahey, L. (1998). Market-Based Assets and Shareholder Value: A Framework for Analysis. *Journal of Marketing, 62(1), 2–18. doi:10.2307/1251799.*

International Conferences on Science and Technology
Natural Sciences and Technology
ICONST NST 2021

Histological and Immunohistochemical Study on the Possible Therapeutic Role of Stem Cells and Curcumin in Cyclophosphamide-induced Cardiotoxicity in Adult Male Albino Rat

Azza Helal[1*]

Abstract: Cyclophosphamide (CP) is used as a chemotherapeutic and an immunosuppressive agent. CP is known to cause multiple organ toxicity; the most obvious is cardiotoxicity.Possibility of therapeutic effect of bone marrow -derived mesenchymal stem cells (BM-MSCs) in ameliorating CP- induced cardiotoxicity compared with Curcumin in albino rats.50 male albino rats were divided into five groups: group I received sterile water injected intraperitoneally; group II received curcumin (200 mg/kg) orally; group III received CP injected once intraperitoneally (200 mg/kg) and were sacrificed on day 40; group IV received the same treatment as group III followed by oral administration of curcumin from day 10 and were sacrificed on day 40; group V received the same treatment as group III followed by a single BM- MSCs injection intraperitoneally at a dose of 1×10^6 cells/ rat on day 10 and were sacrificed on day 40.

Histological structure of the cardiac muscle by light and electron microscopic examination revealed marked structural changes in rats treated with CP alone. Improvement in BM-MSCs group more than curcumin treated group was observed. Immunohistochemical staining of the cardiac muscle showed strong positive immunoreactivity for caspase-3 in group III compared to the control and other groups. Also, BM-MSCs extensively reduced the amount of collagen fibers compared with other groups. The use of curcumin has a little benefical effect on the protection of cardiac muscle against CP toxicity compared with stem cells.

Keywords: Cardiotoxicity; Cyclophosphamide; stem cells ; Curcumin.

1. Introduction

Cardiotoxicity is a serious adverse effect of chemotherapeutic agents [1]. cardiomyocytes have a limited mitotic capacity that cannot support its self-renewal [2]. Cyclophosphamide is an alkylating agent with potent antineoplastic and immunosuppressive properties and possibly the most widely used antineoplastic agent [3]. The metabolism of anti-cancer drugs can lead to more active anti-cancer metabolites but those metabolites can likewise contribute to the observed cardiotoxicity [4]. Bone marrow-derived mesenchymal stem cells (BM-MSCs) are considered the most routinely used in clinical studies because they are easily accessible and are routinely collected from adults without the ethical concern inherent to fetal embryonic tissues [5&6]. Curcumin has been reported to exhibit a strong antioxidant property and acts as a scavenger of free oxygen radicals [7]. This

[1] Faculty of Medicine, Egypt
* Corresponding author: azza.helal2016@gmail.com

study aimed to assess histologically and immunohistochemically the possible protective role and ameliorating effects of BM -MSCs compared with curcumin against cyclophosphamide-induced cardiotoxicity.

2. Materials and methods

Drugs used

- CP (Endoxan vials; Baxter Company, Deerfield, IL, USA) was obtained as vials. Each vial contained 200 mg of CP in dry lyophilized powder form. CP was injected at a dose of 200 mg/kg [8]. The content of one vial was dissolved in 10 ml of sterile water to obtain a concentration of 20 mg/ml for immediate injection. Each rat weighing 200 g was injected with 2 ml of CP.
- Curcumin is available in the market in the form of powder. The dose used in this study was 200 mg/kg orally [9]. The powder was dissolved in 400 ml of sterile water to obtain a concentration of 40 mg curcumin/ml.
- BM-MSCs were prepared in the Department of Medical Biochemistry, Kasr Al-Ainy Faculty of Medicine, Cairo University. They were provided as first-passage culture cells suspended in PBS at a dose of 1×10^6 cells/ rat [8].

Animals

50 albino rats, their weights ranged between 150 and 200 grams, were divided into five groups (10 rats each);

Group I (control): Each rat in this group was intraperitoneally injected once with 2ml sterile water and sacrificed after 10 days. Group II (curcumin-treated): Each rat received 1 ml of the dissolved curcumin powder orally through gastric gavage once daily and sacrificed after 10 days. Group III (CP-treated): Each rat received a single intraperitoneal injection of 2 ml of dissolved CP on the first day of the experiment and were sacrificed on day 40. Group IV (CP plus curcumin): Each rat received a single intraperitoneal injection of CP on the first day of the experiment, followed by oral administration of curcumin from day 10 of the experiment and were sacrificed on day 40. Group V (CP plus BM-MSCs): Each rat received a single intraperitoneal injection of dissolved CP on the first day of the experiment, followed by a single dose of BM-MSCs, injected intraperitoneally on day 10 of the experiment and were sacrificed on day 40.

The experiment took place in Kasr Al-ainy, faculty of medicine, cairo universityand was **approved** by the Local Ethics Committee of the Faculty of Medicine, Cairo University. **Duration of the study** was 40 days from November, 2017 to December, 2017. **Type of the study** is Case / Control study.

Preparation of bone marrow-derived mesenchymal stem cells:

BM was harvested by flushing the tibiae and femora of three 6-weeks-old male Sprague-Dawley albino rats with Dulbecco's modified Eagle's medium supplemented with 10% fetal bovine serum. Nucleated cells were isolated and resuspended in complete culture medium supplemented with 1% penicillin–streptomycin [10]. The cells were incubated at 37°C in 5% humidified CO2 for 12 – 14 days as primary culture. BM-MSCs were distinguished from other BM cells by their tendency to adhere to tissue culture plastic flasks [11]. When they developed (80–90% confluence), the cultures were washed twice with PBS and the cells were trypsinized with 0.25% trypsin for 5 min at 37°C. After centrifugation, the cells were resuspended in serum-supplemented medium and incubated in a culture flask. The resulting culture was referred to as first-passage culture [12]. The second exchange of

medium was done after 6 days when spindle shaped cells appeared with long processes and vesicular nuclei [13]. The hemocytometer was used to determine the total cell count and assess viability of the cells [14]. BM-MSCs in culture were characterized by their adhesiveness and fusiform shape BM-MSCs in culture were characterized by their adhesiveness and fusiform shape under a phase-contrast microscope.

- At the time of injection, the cells were labeled with a PKH26 dye supplied by Sigma, Darmstadt, Germany (PKH26 dye stock, 1 vial containing > 0.1 ml, 1 x 10^{-3} M in ethanol&Diluent C, an iso-osomotic aqueous solution). Their homing in the cardiac tissue was confirmed by immunofluorescence [16] **(Fig. 1)**.

Histological and immunohistochemical study:

The heart of each rat was taken immediately and divided into two specimens.

❖ One was fixed in 10% formol saline solution and was processed to get paraffin sections:

Serial sections of 3-4 microns thickness were cut, mounted on slides and subjected to the following stains:

1) **H&E** stain for general histological examination [17].
2) **Mallory's trichrome** stain for detection of collagen fibers [18].
3) **Immunohistochemical** Staining for caspase -3 antibody (ready- to -use for IHC, catalog code: PA5-23921) using the avidin-biotin-peroxidase complex technique. The primary antibody was a rabbit polyclonal antibody (Thermo Fisher scientific, USA). The dilution used was 1:50 [19&20]. The sections were examined with light microscope and Negative controls were prepared by omitting the primary antibody. Positive tissue control was performed by applying the previous technique in the same way on duodenal specimen (mybiosource.com).

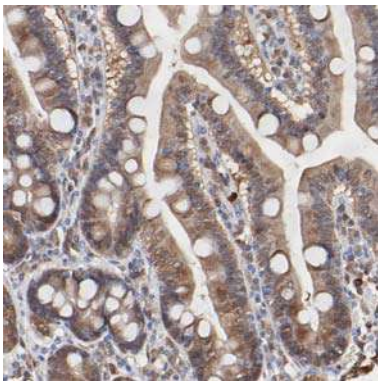

(caspase- 3 immunostaining x 400)

❖ The other specimen was immediately cut into small pieces in all dimensions and fixed in 2.5% buffered glutaraldehyde and was used to prepare ultrathin sections for electron microscopic examination [21].

Morphometric study

The mean area percentage of collagen fibers in Mallory's trichrome-stained sections as well as caspase -3 was measured in 10 non over-lapping high power fields for each animal. Appropriate measurements were taken using the image analyzer computer system (Leica Qwin 500C, Leica, London, UK) [22].

Statistical analysis

The following parameters were expressed as mean ± SD:

(1) Area percentage of collagen fibers in Mallory's trichrome-stained sections.

(2) Area percentage of caspase-3 immunoreaction.

The statistical analysis was carried out using one-way ANOVA analysis of variance for comparison between the different groups, using SPSS (version 16; SPSS Inc., Chicago, Illinois, USA). P values of 0.05 or less were accepted as statistically significant [8].

3. Results

Histological results

Group I (control)

H&E stained sections showed the normal histological structure of cardiac myocytes that appeared arranged in a linear array that branch and anastomose with acidophilic sarcoplasm and oval, centrally located nuclei (Fig.2 a&b). Mallory's trichrome-stained sections showed minimal basophilic collagen fibers surrounding the cardiomyocyte bundles (Fig.2 c). Weak positive immunoreactivity for caspase -3 was observed (Fig.2 d). Ultrastructural examination of ultrathin sections showed the sarcomeres that were bounded on each side by a Z-line with a central dark A-band and two light I-bands in the periphery. A pale H-zone could be seen in the center of A-band bisected by M-line (Fig.2 e&f).

Group II (curcumin treated)

The same structural and ultrastructural results as group I were observed (Fig.3 a&b&c&d).

Group III (CP treated)

H&E stained sections revealed that most of the cardiac muscle fibers were disorganized and lost the normal architecture. Extensive mononuclear cellular infiltrate and diffuse interstitial hemorrhage were also seen. (Fig.4 a & b).

Mallory trichrome stain exhibited strong accumulation of collagen fibers (Fig.4 c) and intense caspase-3 immunoreactivity was seen (Fig.4 d). Ultrastructural examination revealed disturbance of the normal architecture with destruction of myofibrils. Mitochondria appeared swollen with disrupted crista with nuclear indentation (Fig. 4 e&f)

Group IV (CP plus curcumin)

H&E stained sections showed mild restoration of the normal myocardial structure with congestion of blood vessels (Fig.5 a &b). Mallory's trichrome-stain showed mild accumulation of collagen fibers (Fig.5 c). Weak positive immunoreaction for caspase -3 was detected (Fig. 5 d). Ultrastructural examination revealed incomplete recovery of the structural loss with mitochondrial swelling and interstitial haemorrhage. (fig.5 e).

Group V (CP plus BM-MSCs)

H&E stained sections showed nearly complete restoration of the normal histological structure. Few myocardial cells exhibited focal sarcoplasmic vacuolation without obvious nuclear changes together with normal blood vessels and obvious intercalated discs (Figs.6 a&b). Mallory 's trichrome -stain showed mild accumulation of collagen fibers (Fig.6 c). Weak positive immunoreactivity for caspase -3 was encountered (Fig.6 d). Ultrastructural examination revealed obvious amelioration of the degenerative changes. The mitochondria regained their normal linear interposition between the myofibrils with well defined oval or rounded contour. (fig.6 e&f).

Statistical results

Table (1): The mean area % of collagen fibers in all experimental groups.

Groups	Mean	Standard deviation	Significance

Group I	1.2667	.66583	G3 G4 G5
Group II	.7333	.49329	G3 G4 G5
Group III	38.9000	. 2.77308	G1 G2 G5 G6
Group IV	14.2667	1.26623	G1 G2 G3 G4 G5 G6
Group V	3.3333	.92916	G3 G4 G5 G6

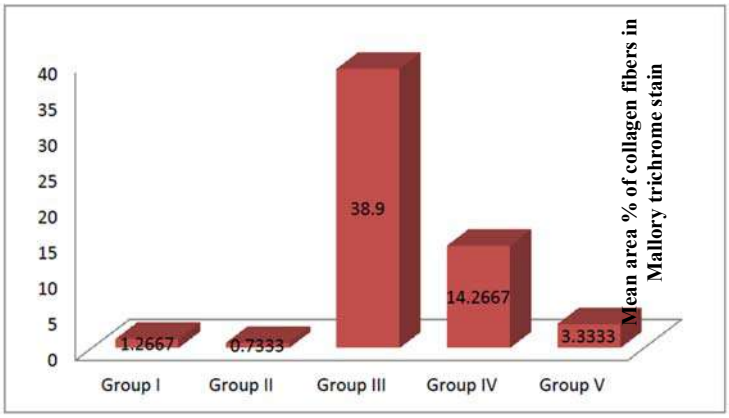

Histogram (1): The mean area % of collagen fibers in all experimental groups.

Table (2): The mean area % of positive immunoreactivity for caspase -3 in all experimental groups.

Groups	Mean	Standard deviation	Significance
Group I	.7500	.55000	G3 G4 G5
GroupII	.8333	.30551	G3 G4 G5
Group III	31.3333	. 3.21455	G1 G2 G3 G4 G5 G6

Group IV	11.0000	1.00000	G1 G2 G3 G4 G5 G6
GroupV	3.0000	1.00000	G3 G4 G5 G6

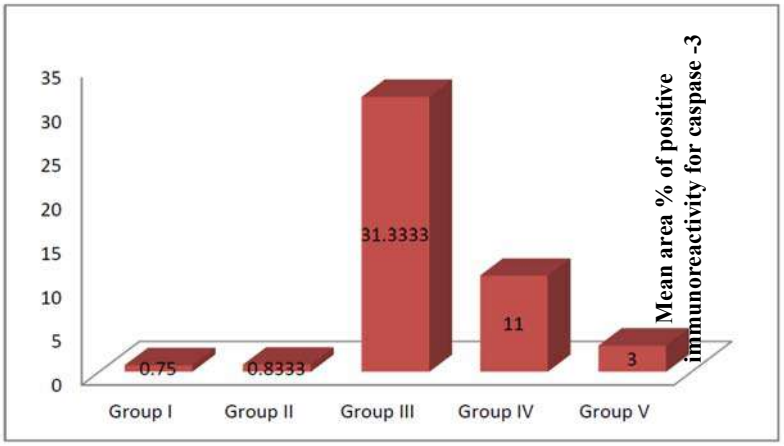

Histogram (2): The mean area % of positive immunoreactivity for caspase -3 in all experimental groups.

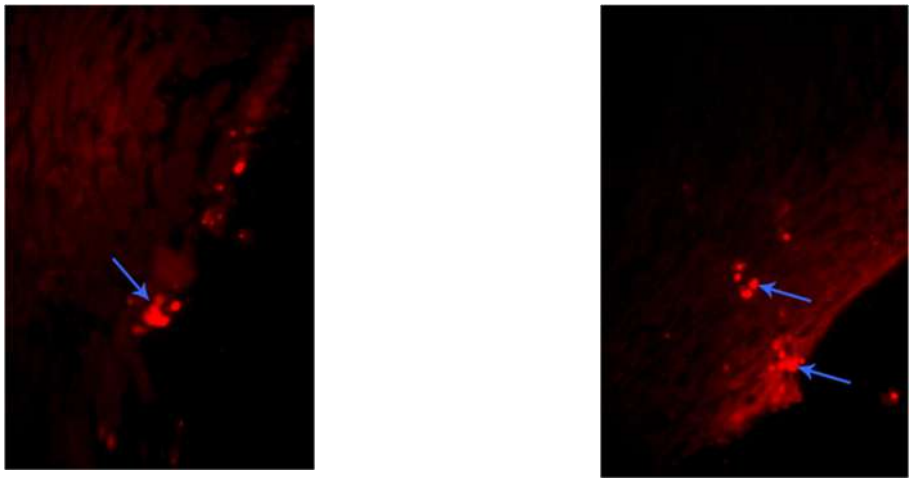

(Fig. 1) A photomicrograph of a section of a rat heart showing positive red immunofluorescent MSCs labelled with PKH26 fluorescent dye (arrows).

) PKH26 immunofluorescence x400 (

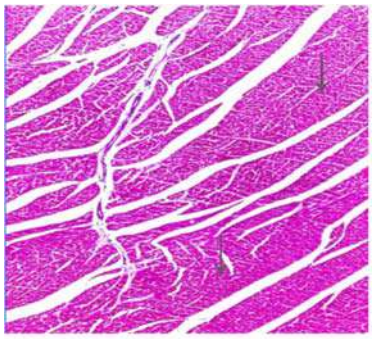

2a

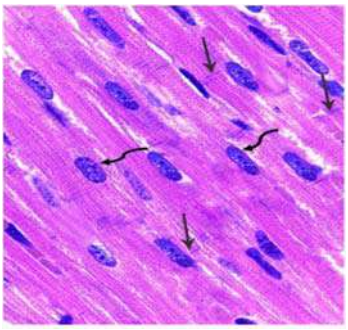

2b

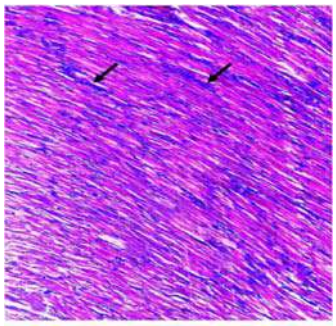

2c

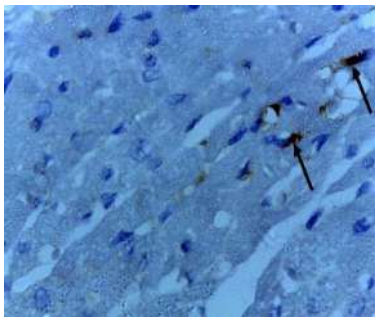

2d

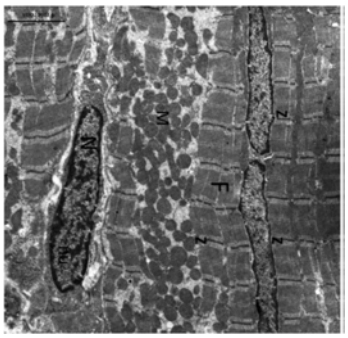

2e

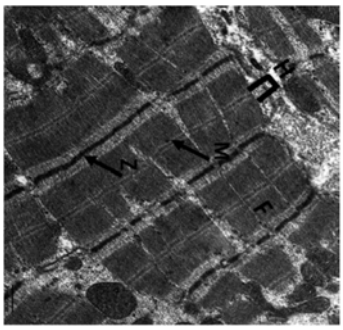

2f

Figure 2. Photomicrographs of sections of the rat myocardium from control group (group I) showing: (a) branched cardiac muscle fibers with acidophilic sarcoplasm (→). (b) centrally located oval nucleus (wavy arrow) and intercalated disc (→). (c) Minimal amount of collagen fibers (→). (d) Weak sarcoplasmic caspase -3 immunoreaction (→). (e) An electron micrograph of a section of cardiac muscle showing a central euchromatic nucleus (N) with prominent nucleolus (nu), parallel arrangement of myofibers (F), the mitochondria (M) arranged in rows between them and regularly arranged sarcomeres between Z lines (Z). (f) regular arrangement of the myofibrils (F) with sarcomeres between Z lines (Z). Notice: H zone (H) bisected by M line (M).

[H&E, (a) ×200/(b) ×1000; Mallory's trichrome, (c) ×200; caspase -3 immunostaining, (d) ×1000; electron micrographs, (e) x 5800/(f) 17500].

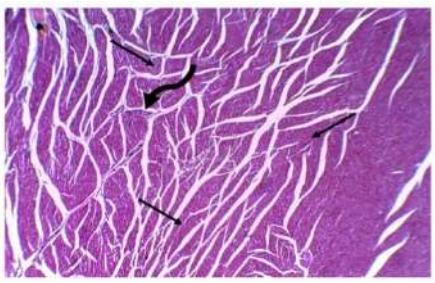

3a

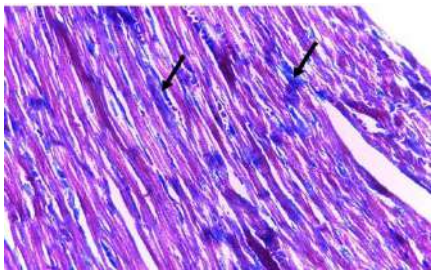

3b

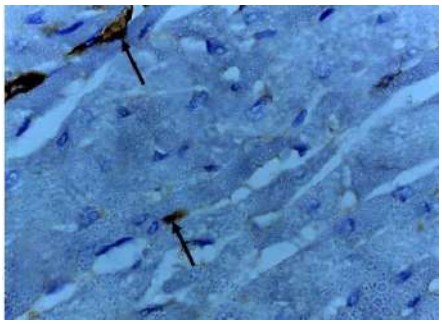

3c

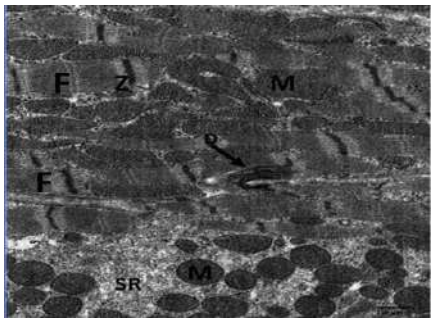

3d

Figure 3. Photomicrographs of sections of rat myocardium from group II (curcumin-treated) showing: (a) branched cardiac muscle fibers with acidophilic sarcoplasm (→) with blood vessels in between (wavy arrow). (b) Minimal collagen fibers (→). (c) Weak sarcoplasmic caspase -3 immunoreaction (→). (d) An electron micrograph showing parallel arrangement of myofibers (F) and the mitochondria (M) in rows between them in association with smooth endoplasmic reticulum(SR). Notice: the regularly arranged Z- lines (Z) and the continuous intercalated disc (D).

[H&E, (a) ×200; Mallory's trichrome (b) ×400; caspase -3 immunostaining, (c) ×1000; electron micrographs, (d) ×5800].

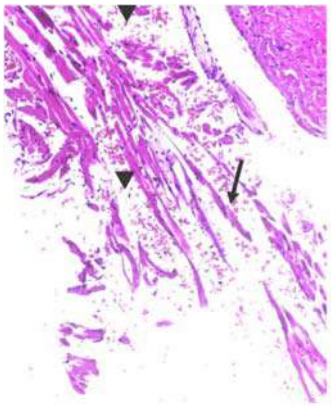

4a

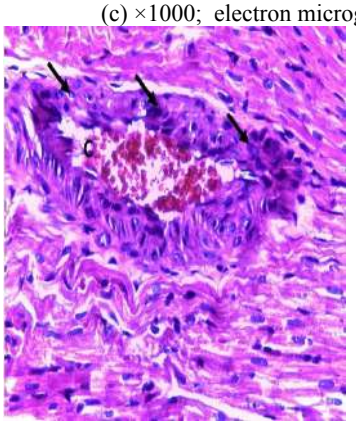

4b

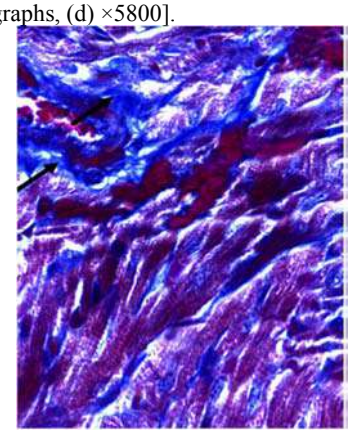

4c

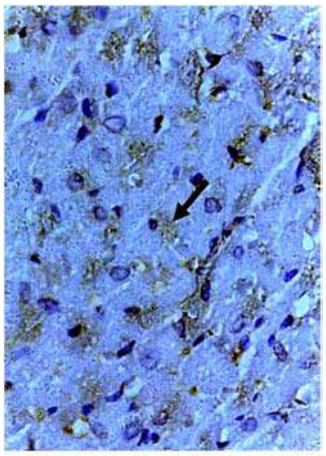

4d

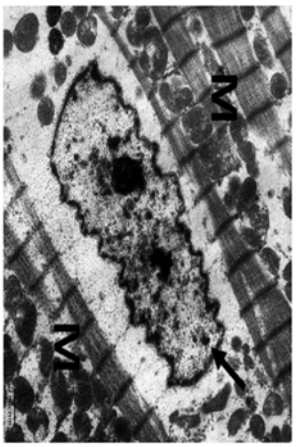

4e

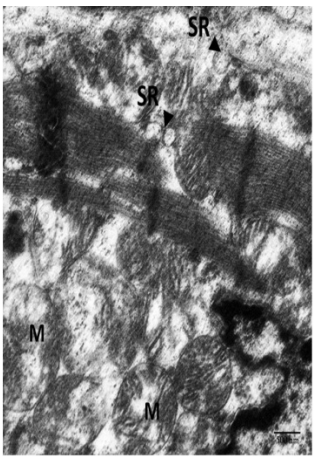

4f

Figure 4: Photomicrographs of sections of rat myocardium from group III showing: (a) fragmentation and disorganization of the cardiac muscle fibers (→) and interstitial haemorrhage (►). (b) congested blood vessels [**C**] and perivascular inflammatory infiltrate (→) were observed. (c) Accumulation of large amount of collagen fibers (→). (d) Intense sarcoplasmic caspase -3 immunoreactivity (→). (e) An electronmicrograph showing degenerated mitochondria with disrupted cristae (M) and indented nucleus with irregular outlines (→).(f) degenerated mitochondria(M) with dilated SR (►).

[H&E, (a) ×200/(b) × 1000; Mallory's trichrome, (c) ×1000; caspase -3 immunostaining, (d) ×1000;

electronmicrograph (e) ×17500/(f) x 20000].

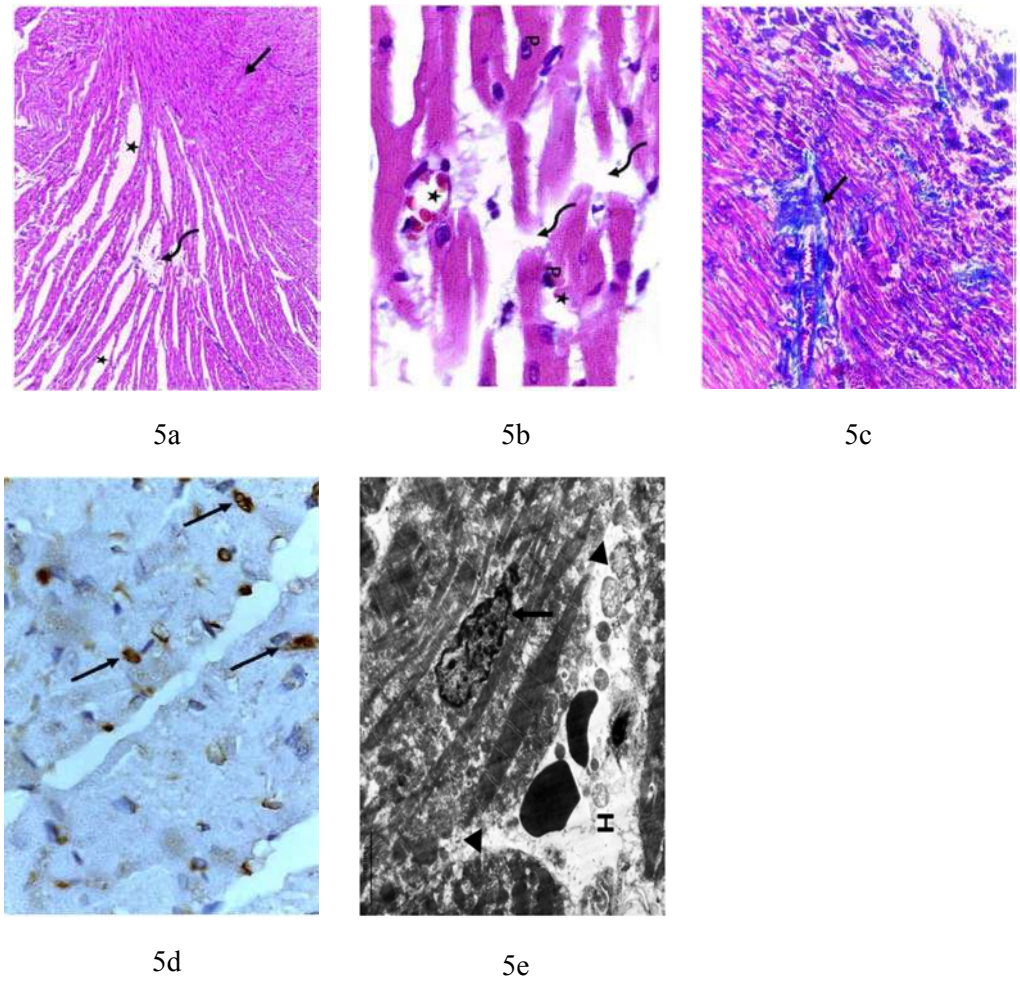

5a 5b 5c

5d 5e

Figure 5: Photomicrographs of sections of rat myocardium from group IV showing (a) prominent fibrillolysis (wavy arrow) and widely spaced cardiac muscle fibers (star), disorganized wavy cardiac muscle fibers (→). (b) splitting of the fibers (wavy arrow), pyknotic nuclei (P) and congested blood vessel (star). (c) moderate amount of collagen fibers in between cardiac muscle fibers (→). (d) moderate sarcoplasmic caspase -3 immunoreactivity. (e) An electronmicrograph showing nuclear indentation (→), areas of fibrillolysis (►)and interstitial haemorrhage (H).

[H&E, (a) ×200/(b) × 1000; Mallory's trichrome, (c) × 400; caspase -3 immunostaining, (d) × 1000; electronmicrograph (e) × 5800].

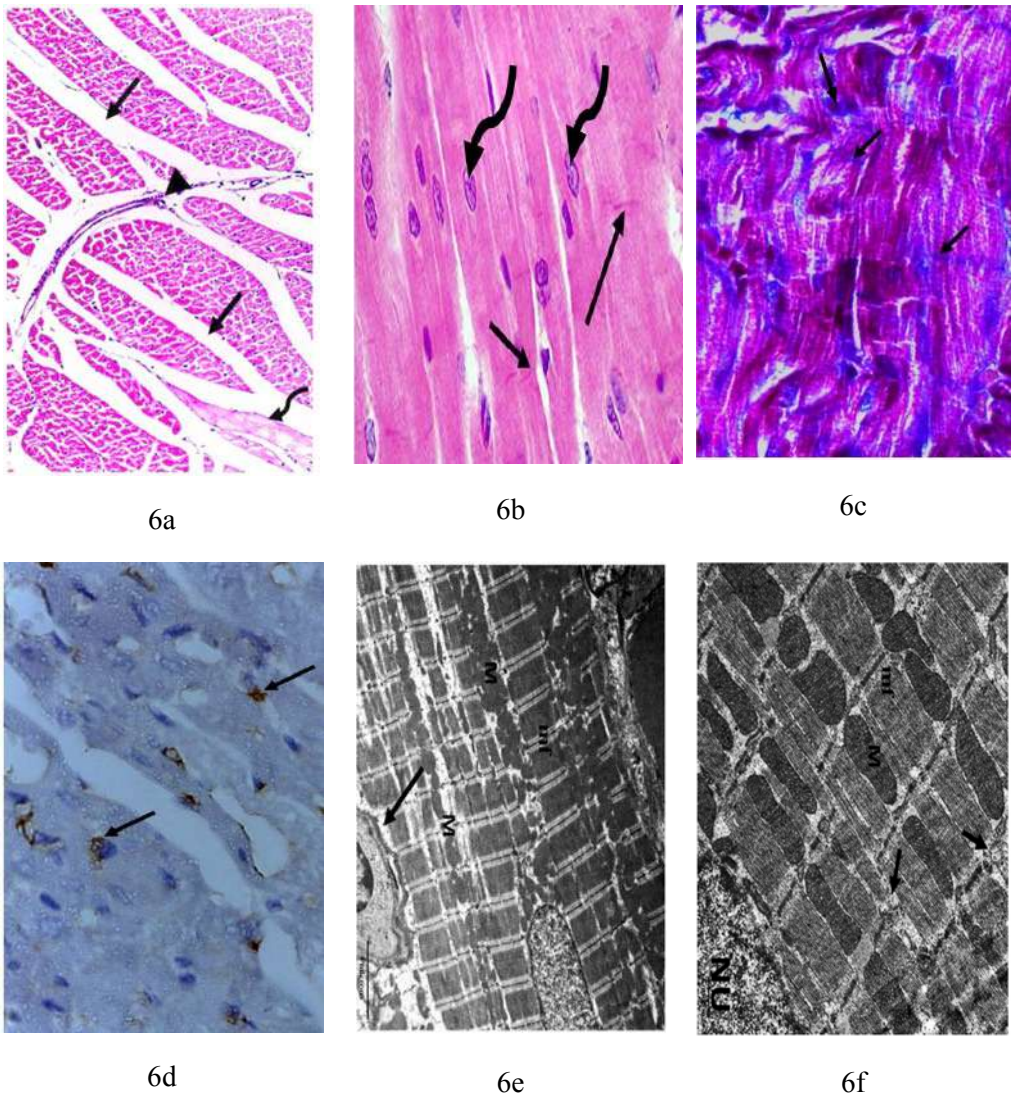

Figure 6: Photomicrographs of sections of rat myocardium from group V showing (a) nearly complete restoration of the normal histological structure with apparently widely spaced muscle fibers (→) with blood vessels inbetween (►) and sarcoplasmic vacuolation (wavy arrow). (b) apparently normal intercalated discs (→) and central oval nucleus (wavy arrow). (c) Mild amount of collagen fibers (arrows). (d) weak sarcoplasmic caspase -3 immunoreactivity (→). (e) An electronmicrograph showing more or less well organized myofibrils (mf), normal mitochondria (M) with apparently normal blood vessel (→). (f) showing a normal euchromatic nucleus (Nu) with dilated smooth Endoplasmic Reticulum (→) and mitochondria (M) arranged between myofibrils (mf).

[H&E, (a) ×200/ (b) × 1000; Mallory's trichrome, (c) × 1000; caspase -3 immunostaining, (d) ×1000; electronmicrograph (e) ×5800 & (f) x17500].

4. Discussion

Cyclophosphamide (CP) is a widely used drug in cancer chemotherapy and immunosuppression, which could cause toxicity of the normal cells due to its toxic

metabolites. The major limitation of CP is the injury of normal tissue, leading to multiple organ toxicity [23&24].

CP itself is not cardiotoxic, rather, the harm is caused by CP metabolites that induce cardiotoxicity through increasing free oxygen radicals and the decrease in the antioxidant defense mechanisms [25].

Oxidative stress has been widely shown to regulate apoptosis and exerts both agonistic and antagonistic effects on apoptotic signaling [26]. It has been demonstrated to mediate p53-dependent cell cycle arrest, DNA repair and apoptosis. [27 &28].

Apoptosis was confirmed in the present work by positive caspase 3 immunoreactivity in all CP -injected rats. So, it can be concluded that both apoptosis and necrosis are aetiological mechanisms that cause CP - induced cardiac injury as previously demonstrated by [29].

In the present work, congestion and apparent dilatation of the blood vessels as well as interstitial hemorrhages were observed. These observations were consistent with [30] who explained these changes to be due to the direct effect of CP on the vascular endothelial cells leading to release of endothelium relaxation factor-nitric oxide (NO).

Interstitial cellular infiltration observed by light and electron microscopic examination was consistent with [31] who reported that CP triggers induction of cytokines that regulate leukocyte trafficking.

The increase of collagen fibrils in the interstitium of myocardium of CP treated animals was explained by [32 &33] who reported that systemic and locally produced neurohumoral factors such basic fibroblast growth factor activate fibroblast proliferation and collagen synthesis. During this study electron microscopic examination revealed markedly affected mitochondria that appeared pleomorphic and disarrayed between myofibrils with distorted cristae. These findings were in accordance with [34 &35&36] who referred these alterations to disruption of calcium homeostasis and inhibition of Na+/K+ -ATPase that induce mitochondrial swelling secondary to intracellular sodium accumulation.

In the MSC-treated group in the current study, there was reduction in the inflammatory cellular infiltration. [37&38] presumed that MSCs attenuate the self inflammatory reaction and enhance the anti-inflammatory reaction by regulating the proliferation and differentiation of immunocytes.

Also in this group, cardiomyocytes showed significant decrease in caspase_ 3 reaction [39] have demonstrated that MSCs protect cardiomyocytes from induced apoptosis through release of cytochrome c from the mitochondria.

Significant decrease in collagen fibers accumulation in MSCs treated group compared with CP treated rats was observed by Mallory trichrome stain and confirmed by statistical analysis which revealed that the mean color area percentage of collagen in MSCs treated group was significantly low and this was concomitant with [40 &41] who mentioned that MSCs exert paracrine anti-fibrotic effects to attenuate myocardial remodelling through regulation of cardiac fibroblasts (CFB) proliferation.

In CP + Curcumin treated group, there was slight improvement. Curcumin fairly attenuated the interstitial fibrosis, this was in consensus with [42&43]. Curcumin also attenuated cardiomyocyte apoptosis and this was in agreement of [44&45] who accused the persistence of most of the histological alterations in this group with no evidence of regaining

the well known picture of the control group to the fact that within limit the cell can compensate for structural derangement , however persistent or excessive injury causes cells to pass the threshold into irreversible injury.

References

1- Asiri, Y. A. (2010). Probucol attenuates cyclophosphamide-induced oxidative apoptosis, p53 and Bax signal expression in rat cardiac tissues. *Oxidative Medicine and Cellular Longevity*, *3*(5), 308-316.

2- Curigliano, G., Mayer, E. L., Burstein, H. J., Winer, E., P. & Goldhirsch, A. (2010). Cardiac toxicity from systemic cancer therapy: a comprehensive review. Progress in cardiovascular diseases, 53(2), 94-104.

3- Ogunsanwo, O. R., Oyagbemi, A.A., Omobowale, T.O., Asenuga, E.R.& Saba, A.B. (2017). Biochemical and electrocardiographic studies on the beneficial effects of gallic acid in cyclophosphamide-induced cardio-renal dysfunction. J Complement Integr Med. Mar 22.

4- Reis-Mendes, A.F., Sousa, E., de Lourdes Bastos, M.& Costa, V.M. (2016). The Role of the Metabolism of Anticancer Drugs in Their Induced-Cardiotoxicity. Curr Drug Metab.;17(1):75-90.

5- Rochefort, Y. G., Vaudin, P., Bonnet, N., Pages, J. C& Charbord, P. & Eder, V. (2015). Influence of hypoxia on the domiciliation of mesenchymal stem cells after infusion into rats: possibilities of targeting pulmonary artery remodeling via cells therapies?. *Respiratory research*, *6*(1), 125.

6- Forte, G., Minieri, M., Cossa, P., Antenucci, D., Sala, M. & Prat, M. (2016). Hepatocyte growth factor effects on mesenchymal stem cells: proliferation, migration, and differentiation. Stem cells, 24(1), 23-33.

7- García-Niño, W.R., & Pedraza-Chaverri, J. (2014). Protective effect of curcumin against heavy metals-induced liver damage. *Food and Chemical Toxicology*, *69*, 182-201.

8- Walaa, M. S. and Laila A. R. (2016). Therapeutic role of bone marrow-derived mesenchymal stem cells in cyclophosphamide-induced cardiotoxicity in adult male albino rat: a morphological and immunohistochemical study. The Egyptian Journal of Histology, 39: 281-293

9- Chakraborty, M.1., Bhattacharjee & A.1., Kamath, J.V. (2017). Cardioprotective effect of curcumin and piperine combination against cyclophosphamide-induced cardiotoxicity. Indian J Pharmacol. 2017 Jan-Feb;49(1):65-70

10- Lennon, D.P.& Caplan, A.I. (2006). Isolation of rat marrow-derived mesenchymal stem cells. Exp Hematol. 2006 Nov;34(11):1606-7.

11- Gnecchi, M. & Melo, L.G. (2009) .Bone marrow-derived mesenchymal stem cells: isolation, expansion, characterization, viral transduction, and production of conditioned medium. Methods Mol Biol. ;482:281-94. doi: 10.1007/978-1-59745-060-7_18.

12- Shu, W., Qingjian, Z., Sisi, L., Quanjun, Z., Li, L. & Liangxue, L. (2019). Conversion of embryonic stem cells into extraembryonic lineages by CRISPR-mediated activators. *Sci Rep* 6, 19648 doi:10.1038/srep19648.

13- Chin, M.H., Mason, M.J., Xie, W., Volinia, S., Singer, M. & Peterson, C. (2009). Induced pluripotent stem cells and embryonic stem cells are distinguished by gene expression . Cell Stem Cell. 2;5(1):111-23. doi: 10.1016/j.stem.2009.06.008.

14- Miri, A., Hashmani, K., Al-aqaba, M., Faraj, L.A., Fares, U & Dua, H.S. (2012). The effect of gravitational force on limbal stem cell growth. Br J Ophthalmol. 2012 Jul;96(7):1034-7. doi: 10.1136/bjophthalmol-2012-301624.
15- Kang, E.J., Byun, J.H., & Park, B.W. (2010). In vitro and in vivo osteogenesis of porcine skin-derived mesenchymal stem cell-like cells with a demineralized bone and fibrin glue scaffold. Tissue Eng Part A. ;16(3):815-27. doi: 10.1089/ten.TEA.2009.0439.
16- Nagyova, M., Slovinska, L., Blasko, J., Grulova, I., Kuricova, M. & Cizkova, D. (2014). A comparative study of PKH67, DiI, and BrdU labeling techniques for tracing rat mesenchymal stem cells. *In Vitro Cellular & Developmental Biology-Animal*, *50*(7), 656-663.
17- Bancroft . J.D. & Gamble, M (2008). Theory and Practice of Histological Techniques, 6th Edition, Churchill livingstone, Elsevier, Mosby, Saunders, P.20 - 200.
18- Wołuń-Cholewa, M., Szymanowski, K., Andrusiewicz, M., Szczerba, A. & Warchoł, J.B. (2010). Trichrome Mallory's stain may indicate differential rates of RNA synthesis in eutopic and ectopic endometrium. Folia Histochem Cytobiol. 2010 Jan 1;48(1):148-52.
19- Jantzie, L.L., Tanay, V.I. and Todd, K.G. (2007). Hand book of Neurochemistry and Molecular Neurobiology. Methods in Immunochemistry, 3 rd edition, chapter 8, Springer, New York, P. 193-218.
20- Almeida, C., Cardoso, M.F., Sousa, M., Viana, P. & Barros, A. (2005). Quantitative study of caspase-3 activity in semen and after swim-up preparation in relation to sperm quality. *Hum Reprod* 20, 1307–1313.
21- Woods, A. & Stirling, J. (2008). Electron microscopy (30) in theory and practice of histological techniques, (editors: Bancroft, J. and Gamble, M), 6th edition, Churchill livingstone, Elsevier, China, P.600
22- Emsley, R., Dunn, G. & White, I.R. (2010). Mediation and moderation of exposure effects in randomised controlled trials of complex interventions. Stat Methods Med Res. 2010;19:237–270.
23- De Jonge, M. E., Huitema, A. D., van Dam, S. M., Beijnen, J., H. & Rodenhuis, S. (2015). Significant induction of cyclophosphamide and thiotepa metabolism by phenytoin. Cancer chemotherapy and pharmacology, 55(5), 507-510.
24- Mythili, Y., Sudharsan, P. T., Selvakumar, E. & Varalakshmi, P. (2004). Protective effect of DL-α-lipoic acid on cyclophosphamide induced oxidative cardiac injury. *Chemico-biological interactions*, *151*(1), 13-19.
25- Kurauchi, K., Nishikawa, T., Miyahara, E., Okamoto, Y., & Kawano, Y. (2017). Role of metabolites of cyclophosphamide in cardiotoxicity. *BMC research notes*, *10*(1), 406.
26- Liu, B., Chen, Y. & Clair, D. K. S. (2008). ROS and p53: a versatile partnership. Free Radical Biology and Medicine, 44(8), 1529-1535.
27- Chaudhari, M., Jayaraj, R., Bhaskar, A. S. B. & Rao, P. L. (2009). Oxidative stress induction by T-2 toxin causes DNA damage and triggers apoptosis via caspase pathway in human cervical cancer cells. *Toxicology*, *262*(2), 153-161.
28- Franco, R., Sánchez-Olea, R., Reyes-Reyes, E. M. & Panayiotidis, M. I. (2009). Environmental toxicity, oxidative stress and apoptosis: menage a trois. *Mutation Research/Genetic Toxicology and Environmental Mutagenesis*, *674*(1-2), 3-22.
29- Todorova, V., Vanderpool, D., Blossom, S., Nwokedi, E., Hennings, L. & Klimberg, V. S. (2009). Oral glutamine protects against cyclophosphamide-induced cardiotoxicity in experimental rats through increase of cardiac glutathione. *Nutrition*, *25*(7-8), 812-817.

30- Ghobadi, E., Moloudizargari, M., Asghari, M.H. & Abdollahi, M. (2017). The mechanisms of cyclophosphamide-induced testicular toxicity and the protective agents. Expert Opin Drug Metab Toxicol. ;13(5):525-536. doi: 10.1080/17425255.2017.1277205.
31- Kurauchi, K., Nishikawa, T., Miyahara, E., Okamoto, Y., & Kawano, Y. (2017). Role of metabolites of cyclophosphamide in cardiotoxicity. *BMC research notes*, *10*(1), 406.
32- ALHaithloul, H. A., Alotaibi, M. F., Bin-Jumah, M., Elgebaly, H. & Mahmoud, A. M. (2019). Olea europaea leaf extract up-regulates Nrf2/ARE/HO-1 signaling and attenuates cyclophosphamide-induced oxidative stress, inflammation and apoptosis in rat kidney. *Biomedicine & Pharmacotherapy*, *111*, 676-685.
33- Borghini, A., Manetti, M., Nacci, F., Bellando-Randone, S., Guiducci, S. &Weber, E. (2015). Systemic Sclerosis Sera Impair Angiogenic Performance of Dermal Microvascular Endothelial Cells: Therapeutic Implications of Cyclophosphamide. Jun 15;10(6):e0130166. doi: 10.1371/journal.pone.0130166. eCollection
34- Park, J. M., Hahn, S. M., Han, J., W. & Lyu, C. J. (2018). A Case of Successfully Treated Severe Heart Failure due to Cyclophosphamide Induced Cardiomyopathy. *Clin Pediatr Hematol Oncol*, *25*(1), 71.
35- Iqubal, A., Iqubal, M.K., Sharma, S., Ansari, M.A. & Haque, S.E. (2019). Molecular mechanism involved in cyclophosphamide-induced cardiotoxicity: Old drug with a new vision. PLife Sci. 1;218:112-131. doi: 10.1016/j.lfs.2018.12.018.
36- El-Agamy, D. S., Elkablawy, M. A. & Abo-Haded, H. M. (2017). Modulation of cyclophosphamide-induced cardiotoxicity by methyl palmitate. Cancer chemotherapy and pharmacology, 79(2), 399-409.
37- Rosen, O., Massenkeil, G., Hiepe, F., Pest, S. & Arnold, R. (2001). Cardiac death after autologous stem cell transplantation (ASCT) for treatment of systemic sclerosis (SSc): no evidence for cyclophosphamide-induced cardiomyopathy. Bone marrow transplantation, 27(6), 657.
38- Rog-Zielinska, E. A., Norris, R. A., Kohl, P. & Markwald, R. (2016). The living scar–cardiac fibroblasts and the injured heart. Trends in molecular medicine, 22(2), 99-114.
39- AdiwinataPawitan, J. (2019). Exploring the Most Promising Stem Cell Therapy in Liver Failure: A Systematic Review. Stem Cells Int. 2019 Dec 1;2019:2782548. doi: 10.1155/2019/2782548.
40- Wysoczynski, M., Bolli, R. (2019). A realistic appraisal of the use of embryonic stem cell-based therapies for cardiac repair. Eur Heart J. 2019 Nov 28. pii: ehz787. doi: 10.1093/eurheartj/ehz787.
41- Wen, Z., Zheng, S., Zhou, C., Wang, J. & Wang, T. (2011). Repair mechanisms of bone marrow mesenchymal stem cells in myocardial infarction. *Journal of cellular and molecular medicine*, *15*(5), 1032-1043.
42- Liu, K., Chen, H., You, Q. S., Ye, Q. & Lu, Q. (2017). Curcumin attenuates myocardial ischemia–reperfusion injury. *Oncotarget*, *8*(67), 112051.
43- He, Y.C., He, L., Khoshaba, R., Lu, F.G., Cai, C. & Cao, D. (2019). Curcumin Nicotinate Selectively Induces Cancer Cell Apoptosis and Cycle Arrest through a P53-Mediated Mechanism.Molecules.18;24(22). pii: E4179. doi: 10.3390/molecules24224179.
44- Ma, J., Ma, S.Y. & Ding, C.H. (2017). Curcumin reduces cardiac fibrosis by inhibiting myofibroblast differentiation and decreasing transforming growth factor β1 and matrix metalloproteinase 9/tissue inhibitor of metalloproteinase 1. Chinese journal of integrative medicine, 23(5), 362-369.

45- Altenburg, J.D., Bieberich, A.A., Terry, C., Harvey, K.A. & Siddiqui, R.A. (2011). A synergistic antiproliferation effect of curcumin and docosahexaenoic acid in SK-BR-3 breast cancer cells: unique signaling not explained by the effects of either compound alone. *BMC cancer*, *11*(1), 149.

المستخلص

المقدمة: يستخدم عقار السيكلوفوسفاميد على نطاق واسع كعلاج كيميائي وعامل مثبط للمناعة أثناء عملية زرع الأعضاء. ويعد عقار السيكلوفوسفاميد من العقاقير الأولية الغير نشطه؛ والّذي يتم تحويله في الكبد إلى مركبات أكثر نشاطا لها تأثير علاجي كيميائي . وعلى الرغم من الاستخدامات السريرية المتعدده ، فمن المعروف أن السيكلوفوسفاميد يتسبب فى احداث سمية أعضاء متعددة ؛ وتعد سمية القلب هى الأكثر وضوحا من بينهم.

الهدف من الرسالة: وقد أجريت هذه الدراسة لبحث دور الخلايا الجذعية المشتقة من نخاع العظام الوسيطة مقارنة" بالكركمين في علاج سمية القلب النسيجية الناتجة عن عقار سيكلوفوسفاميد

مادة و طرق البحث: تم تقسيم الفئران البيضاء البالغه والتى يبلغ عددها خمسون فأرا" إلى خمسة مجموعات: المجموعة الأولى استخدمت كمجموعه ضابطه. المجموعة الثانية تلقت الكركمين المذاب عن طريق الفم(200 مجم / كجم من وزن الجسم). المجموعة الثالثة تلقت جرعة واحدة من السيكلوفوسفاميد 200 مجم / كجم من وزن الجسم) عن طريق الحق البريتونى في اليوم الأول من التجربه وتم التضحية بهم في اليوم الأربعون؛ المجموعة الرابعة وقد تلقت نفس علاج المجموعة الثالثة تلاها تناول الكركمين من اليوم العاشر وتم التضحية بهم في اليوم الأربعون. وأخيرا تلقت المجموعة الخامسة نفس علاج في اليوم 10 وتم التضحية بهم في اليوم 40. الخلايا الجذعيه المجموعة الثالثة تلاها حقن

النتائج: كشف الفحص المجهري الضوئى والإلكترونى لمقاطع عضلة القلب عن حدوث تغييرات نسيجيه ملحوظة في الفئران التي عولجت بالسيكلوفوسفاميد وحده (المجموعه الثالثه). وكانت هذه التغييرات في شكل تضخم الخلايا مع ظهور فجوات سيتوبلازية، وتغيرات نووية وتسلل خلوي وكذلك الشعيرات الدموية المحتقنة. أليلف الكولاجين صوحبت ايضا بزيادة كبيرة والتغيرات المورفولوجية الميتوكوندرية وتحسنت تلك التغييرات بشكل كبير في المجموعة التى تم حقنها بالخلايا الجذعيه أكثر من التي أظهرت caspase -3تلك التى تلقت الكركمين. لقد اثبت موت الخلايا المبرمج بالدراسة المناعية من زيادة ملحوظة مع حقن السيكلوفوسفاميد ، ولكن انخفضت مع العلاج بالخلايا الجذعية .

والخلاصة: إن استخدام الكركمين قد يكون له تأثير ضئيل على حماية عضلة القلب ضد سمية عقار السيكلوفوسفاميد مقارنة بالخلايا الجذعيه .

International Conferences on Science and Technology
Natural Sciences and Technology
ICONST NST 2021

Surfactant-Supported Separation and Removal of Pb(II) ions from the Multi-component System Through Liquid Membranes

Jasmin Suljagić[1*], Mersiha Suljkanović[1], Edita Bjelić[1], Azra Kovačević[1]

Abstract: A chloroform membrane system with dicyclohexano-18-crown-6 was applied for selective removal of Pb(II) ions from an aqueous source phase containing Pb(II), Ni(II), Zn(II), Co(II), Cu(II) and Cd(II) metal cations into an aqueous receiving phase. The selectivity and efficiency of Pb(II) ions removal in the presence of metal cations as competing ions in a multi-component aqueous source phase were investigated. The influence of the oleic and palmitic acid as supporting surfactants in the membrane phase on the removal of Pb(II) ions was also analyzed. Metal ions concentration in aqueous phases was monitored by flame atomic absorption spectrophotometry, after 3 hours of membrane transport. Removal of Pb(II) ions was achieved without significant reduction in the efficiency compared to the liquid membrane transport of a single-component system. Efficiencies of more than 80% for Pb(II) removal were obtained. It was found that none of the presence cations, interfered with Pb(II) removal. The presence of fatty acids increases the efficiency of removed Pb(II) ions into the receiving phase. By reducing the Pb(II) ions concentration in the source phase, the Pb(II) removal into the receiving phase increases to 97 %.

Keywords: heavy metals, Pb(II) removal, crown ether, oleic acid

1. Introduction

Water pollution due to the discharge and accumulation of heavy metals has become one of the most serious problems in the world. Heavy metals are usually present in trace amounts in natural waters, but many are toxic even at very low concentrations (Akif et al., 2002). Since lead in small quantities is primarily an industrially important element and an environmental pollutant, controlling lead in the environmental samples is of major importance (Eslami et al., 2011). The separation of metal cations from complex matrices of other species is of critical importance in analytical chemistry, and especially in industrial processes. In addition to finding the most efficient and reliable quantitative methods, for determining undesirable components, attention is focused on removal these components from the environment. New technologies in wastewater treatment are precisely membrane processes. Liquid membrane is known as a green technology because of its green characteristics such as being eco-friendly and its low consumption of organic solvent (Chang et al., 2010). A liquid membrane system involves an organic liquid membrane that serves as a semipermeable barrier between two aqueous phases, the source phase (SP) and receiving phase (RP). In this method, solute species dissolve in the membrane and diffuse across the membrane due to an imposed concentration gradient (Baker et al., 2004). Polyether ligands are among the most suitable

[1] University of Tuzla, Faculty of Technology, Departmant of Organic Chemistry, Tuzla, Bosnia and Herzegovina [2]

* Corresponding author: jasmin.suljagic@untz.ba

host molecules for many metal ions, due to the presence of oxygen atoms as electron donors in their structure, which enables the formation of coordination-covalent bonds. The interaction of the ligand and metal cation depends on the nature of the metal cation but also depends on the number, distance, and orientation of the donor atoms of the ligand that are structurally accessible to the complexed cation (Salman et al.,1996). The Pb(II) ions are removed from the source phase (SP) to the receiving phase (RP) via a chloroform membrane phase (MP). The movement of charged species (carrier-metal complex) through the hydrophobic liquid membrane is accomplished by the presence of a large lipophilic anion, such as picrate, in the source phase (Kazemi et al., 2005). After complexation of the carrier with Pb(II) ion on the left side of the membrane (DC18C6-Pb^{2+}), $(Pic^{-})_2$ ion-pair is formed at the SP-MP interface and diffuses down its concentration gradient within the organic phase. On the right side of the membrane, at the MP-RP interface, the metal ion would be released into the receiving phase via the formation of ternary adducts (carrier-metal ion-stripping agents/carrier-metal ion-surfactants). At this stage, the free carrier diffuses back across the liquid membrane and the Pb(II) removal cycle. Based on this assumption, the mechanism for metal ion transport was proposed (Malihe et al., 2010).

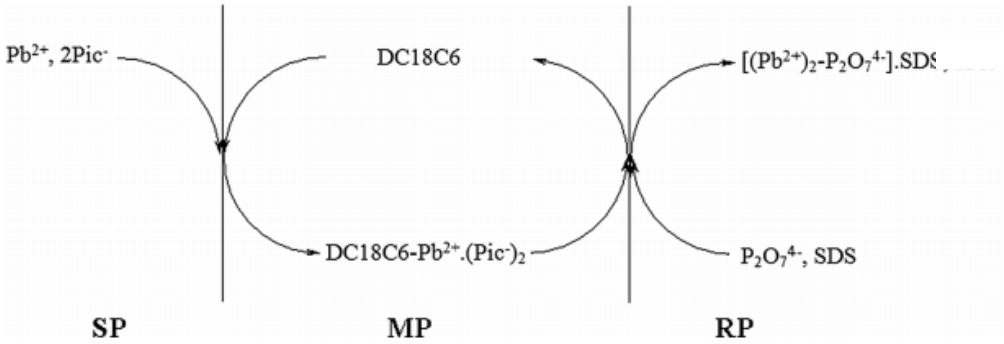

Figure 1. Proposed mechanism of metal ion transport through an organic liquid membrane containing dissolved ligand (L), from SP (contains: M^{2+} cations and counterions picrate Pic^{-}) to RP

In this paper, we studied the efficiency of Pb(II) removal from an aqueous solution in the presence of Ni(II), Zn(II), Co(II), Cu(II), and Cd(II) ions as competing ions in a multi-component aqueous source phase through the bulk liquid membrane system. In the presence of picrate ion as a hydrophobic counter ion in the source phase and disodium-EDTA ion as a selective stripping agent and Triton X-100 as a suitable synergistic co-stripping agent in the receiving phase, the Pb(II) ion found to transport selectively and quantitatively across the chloroform bulk liquid membrane in 3 h. The addition of fatty acids to the membrane phase leads to better transport efficiency.

2. Material and Method

For every transport experiment, two aqueous solutions and one non-aqueous organic solution (membrane), were prepared, as follows.

Source solutions were prepared from:

- Standard Pb(II), Ni(II), Zn(II), Co(II), Cu(II) and Cd(II) solution (1000 mg/L), Merck

- Picric acid ($C_6H_3N_3O_7$), c = $1 \cdot 10^{-3}$ mol/L, 99%, Kemika
- Acetate buffer solution (pH=5), prepared from CH_3COOH (purris. p.a., Fluka) and NaOH (g.r., Merck)
- Formic acid bufffer solution (pH=3), prepared from HCOOH and NaOH (g.r., Merck)

Organic solutions were prepared from:

- Organic solvents: chloroform ($CHCl_3$)
- Macrocyclic ligands: dicyclohexano-18-crown-6 (DCH18C6)

Receiving solution were prepared from:

- Triton X-100 surfactant ($1{,}4 \cdot 10^{-3}$ mol/L)
- Disodium-EDTA ($1 \cdot 10^{-3}$ mol/L)
- Acetic acid buffer solution (pH=5), prepared from CH_3COOH (purris. p.a., Fluka) and NaOH (g.r., Merck).

Transport Procedure

Cylindric glass container, i.e. "transport cell", with inner diameter of 5 cm and central glass tube (2 cm in diameter), have been used for this study (Figure 2.).

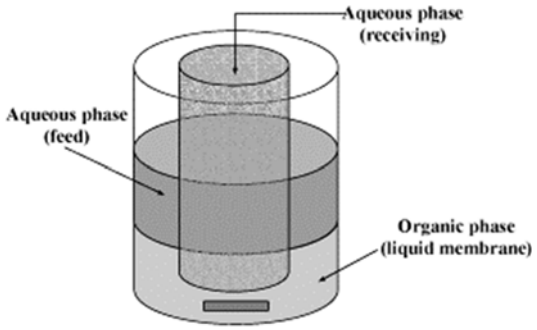

Figure 2. Scheme of a cylindrical glass vessel, "transport cell" (Fahmideh et al., 2010)

Central tube provides physical separation of two aqueous phases: source phase (SP), and receiving phase (RP). Membrane phase (MP) lies under the aqueous phases and connects them. The source phase (SP) contained 10 mL of a mixture of tested Pb(II) ions ($1 \cdot 10^{-4}$mol/L, $1 \cdot 10^{-3}$mol/L and $2{,}5 \cdot 10^{-4}$mol/L) and metal cations Ni(II), Zn(II), Co(II), Cu(II), Cd(II) ($1 \cdot 10^{-3}$mol/L). The receiving phase (RP), which is outside the central tube, contained a stripping agent. The membrane phase (MP) contained 50 mL of a suitable ligand ($1 \cdot 10^{-3}$mol/L) dissolved in an organic solvent; the membrane layer lies beneath the aqueous phases and connects them. The membrane phase is mixed with a magnetic stirrer so that under these conditions the contact surfaces between the aqueous phases are straight and precisely defined (Nipamanjari et al., 2010). pH measurements of aqueous solutions were performed using the pH meter (GLP31 Crison Instruments). Quantification of metal ions removed during the transport experiments was obtained by Flame Atomic Absorption Spectrometry technique, using the instrument Perkin Elmer AAnalyst 200.

3. Results

The selectivity of the process towards Pb(II) ions was tested by performing the transport of Ni(II), Zn(II), Co(II), Cu(II), Cd(II) metal cations containing Pb(II) ions in their mixtures. The results of the measured content of removed Pb(II) ions in the source and final phase, and calculated for the membrane phase, for the among different mixture are summarized in Table 1. It was found that even in the presence of these metal ions with respect to Pb(II) ion, there is no serious interference in the transport process of this heavy metal ion. From the results showed in Table 1. the uptake from the SP is evident for all systems, and removal of Pb(II) ions was achieved without significant reduction in the efficiency compared to the liquid membrane transport of a single-component system, approximately 80 % removed Pb(II) ions for all measuring systems. Formed DC18C6-Pb^{2+} complex has a proper formation constant (log Kf = 4.43 in water) which is within the optimum range necessary for uphill transport (Lamb et al., 1980). Dicyclohexano-18-crown-6 (DC18C6) due to its very lipophilic character and its corresponding cavity size for selective complexation with Pb(II) ion proved to be a selective and efficient carrier for Pb(II) removal via BLM. The extraction of Pb(II) ions from the source phase (SP) into the membrane phase (MP) is a relatively easier process compared to the re-extraction from MP to RP, although the formation of stable complexes with DC18C6, could results in high extraction efficiency into the MP, either their too high stability and/or low affinity for stripping agents in RP prevents their convenient release into the aqueous phase.

Table 1. Amount of Pb(II) ions removed from various mixtures through a bulk liquid membrane system; source phase: $1 \cdot 10^{-3}$mol/L mixture of metal ions and $1 \cdot 10^{-3}$mol/L picrates; organic solvent chloroform contained $1 \cdot 10^{-3}$mol/L of DCH18C6; receiving phase: Triton X-100 surfactant ($1{,}4 \cdot 10^{-3}$mol/L) disodium-EDTA ($1 \cdot 10^{-3}$mol/L)

Mixture	% Pb(II)			
	RP	MP	SP	REMOVED
Pb^{2+}	40.8	41	19	81.8
Pb^{2+}+Ni^{2+}	37.8	43	19.2	80.8
Pb^{2+}+Ni^{2+}+Co^{2+}	57.1	23	19.9	80.4
Pb^{2+}+Ni^{2+}+Co^{2+}+Zn^{2+}	46.5	32	21.4	78.5
Pb^{2+}+Ni^{2+}+Co^{2+}+Zn^{2+}+Cd^{2+}	60.3	18	21.7	78.3

Effect of surfactants on cation transport

Surfactant systems have been recognized as very useful alternatives for improving analytical methodologies and the development of new concepts in analytical chemistry (Hinze et al., 1984, Plizzetti and Pramauro, 1985). Adding a long chain fatty acid reduces the degree of carrier loss and could have a cooperative effect in the uphill transport of the metal cation through the ligand membrane. A possible reason for this cooperative behavior would be existence of some proton donor–acceptor interaction between the lipophilic fatty acid (as proton donor) and the donor atoms of the ligand (as proton acceptor), which can impart a greater degree of lipophilicity to the ligand–metal ion complex, in order to facilitate the cation transport through the liquid membrane (Dadfarnia and Shamsipur, 1992).

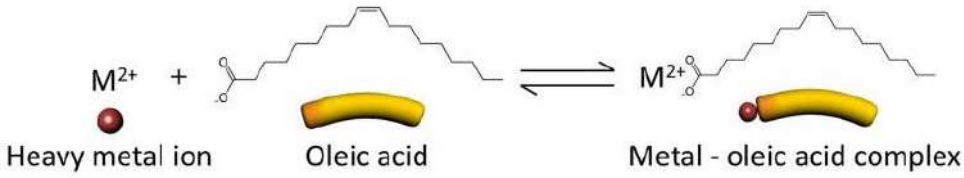

Figure 3. Schematic illustration of the spontaneous phase transfer-mediated selective removal of heavy metal ions using oleic acid

The influence of the palmitic acid and oleic acid as surfactant ($1 \cdot 10^{-3}$ mol/L) in the membrane phase containing a known concentration of the carrier ($1 \cdot 10^{-3}$ mol/L) and organic solvents (chloroform) on the removal of Pb(II) ions was also investigated. The results are summarized in Figure 4. As is evident, the efficiency of Pb(II) ions removal measured in receiving phase increases in the presence of the surfactants in chloroform as liquid membranes. Results measured in receiving phase showed the highest removal of Pb(II) ions (65%) obtained with DCH18C6 as a ligand in the organic phase supported by palmitic acid. Removal of Pb(II) ions was achieved without significant reduction in the efficiency (63%) for the same system supported by oleic acid. This may be due to the formation of hydrogen bonds between the donor atoms of the ligand and the acidic proton of the carboxylic acids in these solvent systems which results in the formation of a weaker complex between the Pb(II) ion and the ligand in the presence of these fatty acids.

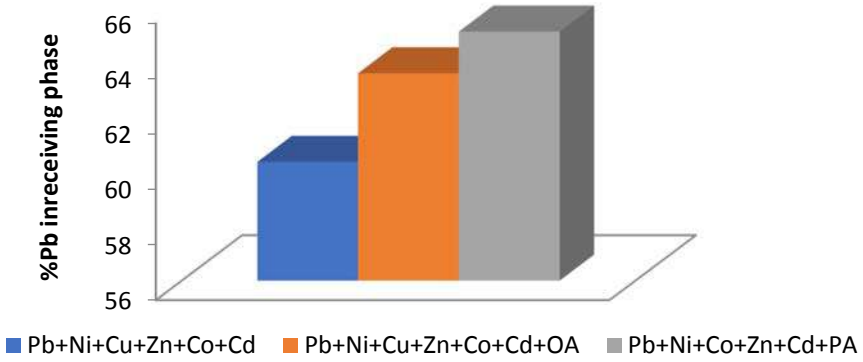

Figure 4. Comparison of the Pb(II) removal efficiencies in presence of oleic acid (OA) and palmitic acid (PA) (source phase: $1 \cdot 10^{-3}$mol/L mixture of metal ions and $1 \cdot 10^{-3}$mol/L picrates; organic solvent chloroform contained $1 \cdot 10^{-3}$mol/L of DCH18C6; receiving phase: Triton X-100 surfactant ($1{,}4 \cdot 10^{-3}$mol/L) disodium-EDTA ($1 \cdot 10^{-3}$mol/L)

Effect of Pb(II) ion concentration in SP on transport process

The effect of Pb(II) ions concentration in the source phase on Pb(II) ions removal under optimal experimental conditions was investigated and the results are shown in Table 2. As seen, the removal efficiency is increased with decreasing concentration of Pb(II) ions in the source phase. It may be due to the carrier loading effect in the membrane (Alpoguz et al., 2005). Optimal transport conditions were obtained for a system with decreasing concentration supported by oleic acid. The excellent efficiency and high degree of selectivity for the Pb(II) ions showed a system with lowest concentration of Pb(II) ions in source phase with more than 97% removed Pb(II) ions.

Table 2. Effect of Pb(II) concentration in SP on the Pb(II) removal
SP, 10 mL of varying concentration of Pb(II) ($1\cdot10^{-4}$ mol/L, $1\cdot10^{-3}$mol/L and $2{,}5\cdot10^{-4}$ mol/L)
MP, 50 mL of $1\cdot10^{-3}$mol/L DC18C6 in chloroform with oleic and palmitic acid ($1\cdot10^{-3}$mol/L)
RP, Triton X-100 surfactant with disodium-EDTA

Mixture	Pb(II), mg/L	Surfactant assisted	% of removed Pb(II) ions
$Pb^{2+}+Ni^{2+}+Co^{2+}+Zn^{2+}+Cd^{2+}$	$1\cdot10^{-3}$	Oleic acid	60
$Pb^{2+}+Ni^{2+}+Co^{2+}+Zn^{2+}+Cd^{2+}$	$2{,}5\cdot10^{-4}$	Oleic acid	54
$Pb^{2+}+Ni^{2+}+Co^{2+}+Zn^{2+}+Cd^{2+}$	$1\cdot10^{-4}$	Oleic acid	97

Discussion and Conclusions

The present study showed that DCH18C6 ether is an excellent carrier for selective and efficient removal of Pb(II) ions through chloroform as an organic solvent. Removal of Pb(II) ions from different mixtures was achieved without significant reduction in the efficiency compared to the liquid membrane transport of a single-component system. The presence of fatty acids increases the efficiency of removed Pb(II) ions into the receiving phase. The effect of decreasing concentration of Pb(II) ions in the source phase reflected with increased efficiency removed Pb(II) ions in the receiving phase. High efficiency and selectivity of the Pb(II) ions removal through the designed membrane system revealed its potential application to the selective and efficient removal and purification of the cation in real samples of complex matrices.

References

Akif, M., Khan, A. R., Sok, K.,(2002). Textile effluents and their contribution towards aquatic pollution in the Kabul River (Pakistan). Journal of the Chemical Society of Pakistan, 24(2) 106–111.

Eslami, S., Moghaddam, A. H., Jafari, N., Nabavi, S. F., Nabavi, S. M., and Ebrahimzadeh, M. A.(2011). Trace element level in different tissues of *Rutilus frisii* kutum collected from Tajan river, Iran. Biological Trace Element Research. 14(2), 965–973.

Chang, S. H., Teng, T. T., Ismail, N.2010 Extraction of Cu(II) from aqueous solutions by vegetable oil-based organic solvents, J. Hazard. Mater. 181 (2010) 868–872.

Baker, R.(2004). Membrane Technology and Applications, John Wiley & Sons Ltd.: New York, USA, 2004

Salman, S.R., Derwish, G.A.W., Al-Marsoumi, S.M.H. (1996) Journal of Inclusion Phenomena and Molecular Recognition in Chemistry, 25 295-302

Kazemi, S.Y., & Shamsipur, M.(2005). Selective Transport of Lead(II) through a Bulk Liquid Membrane Using a Cooperative Carrier Composed of Benzylaza-12-crown-4 and Oleic Acid. Bulletin of the Korean Chemical Society. 26(6). 930-934

Malihe, S. Kazemi, Golamhossein Rounaghi. (2010). Highly selective transport of lead cation through bulk liquid membrane by macrocyclic ligand of decyl-18-crown-6 as carrier, Russian Journal of Inorganic Chemistry, 55: 12 (2010) 1987–1991

Fahmideh-Rad E., Rounaghi GH., Arbab Zavar MH., Chamsaz M. (2010) Spectrometric determination of Pb2+ cation after selective bulk liquid membrane transport using benzo-18-crown-6 as carrier. Der Pharma Chemica 2(6):8-18.

Nipamanjari, D., Sanjib, B., Mukherjee, A.K. (2010). Charge transfer complex formation between TX-100/CCl4. Molecular Physics 108 (11), 1505– 1511

Lamb, J.D., Chritensen, J.J., Oscarson, J.L., Nielsen, B.L., Asay, B.W., Izatt R.M.(1980) J. Am. Chem. Soc. 102. 6820

Hinze, W.L., Singh, H.N., Baba, Y., Harvey, N.G.1984. Micellar enhanced analytical fluorimetry.Trends in Analytical Chemistry 3(8) 193–199

Plizzetti, E., Pramauro, E., 1985. Analytica Chimica Acta 169, 1–29

Dadfarnia, S., Shamsipur, M. 1992. Highly Selective Membrane Transport of Zn^{2+} Ion by a Cooperative Carrier Composed of 1,10-Diaza-18-crown-6 and Palmitic Acid. Bulletin of the Chemical Society of Japan 65(10). 2779–2783.

Alpoguz, H. K.; Memon, S.; Ersoz, M.; Yilmaz, M.(2002). Transport of metals through a liquid membrane containing calix[4]arene derivatives as carrier. Sep. Purif. Technol. 37(9), 2201-2215